Gabor methods for imaging

Michael P.Lamoureux *
University of Calgary

Joint work with P. Gibson, G. Margrave

Fields Workshop on Microlocal Methods in Medical Imaging

.

August 13–17, 2012

Abstract

The Gabor transform of a signal creates a time-frequency representation of physical data which can be directly manipulated through multiplication by symbols, analogous to the action of pseudodifferential operators and their representation through symbols in the time-frequency domain.

This two-lecture minicourse describes the basics of Gabor transforms and Gabor multipliers, windowing considerations, representation of linear operators including differential operators, and the use of Gabor multipliers in nonstationary filtering, deconvolution, and numerical wave propagation. Some particular imaging applications are described.

OUTLINE

Part I Imaging

Gabor transforms
Gabor multipliers
Windows
Gabor deconvolution
Gabor filtering in 2D

Part II

Discrete Gabor methods
Frame theory
Wave propagators
Gabor functional calculus
Minimum phase
Conclusion

Notes on Online Posting of this Talk

The original talk included several animations, movies, and sound clips. These were too long to include in the online edition, so have been removed. The reader will just have to click past the animations. Apologies.

Imaging

The focus of this workshop is on medical imaging. For example, here is a TSAR model used for microwave imaging in breast tumour detection.

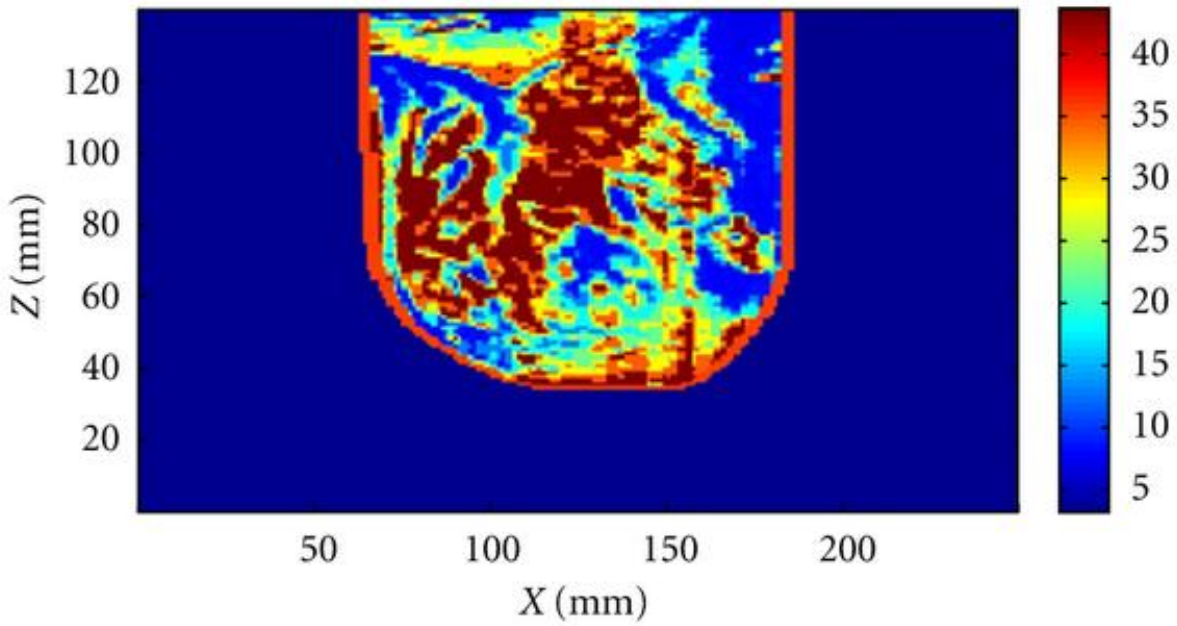

Figure 1: Model for Tissue Sensing Adaptive Radar Imaging (TSAR)
– courtesy Dr. Elise Fear, University of Calgary

The unusual shape of the model comes from the set of the TSAR imager:

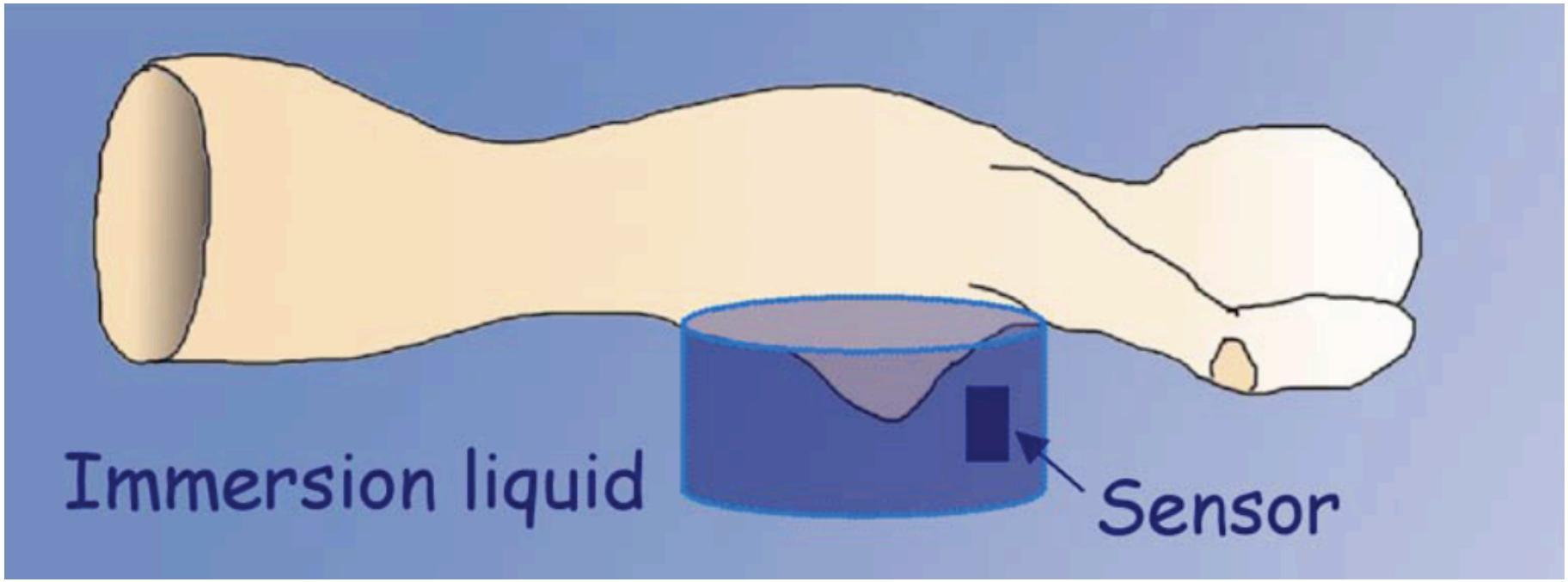

Figure 2: Equipment setup for Tissue Sensing Adaptive Radar Imaging (TSAR) – from M. Stuchly, University of Victoria

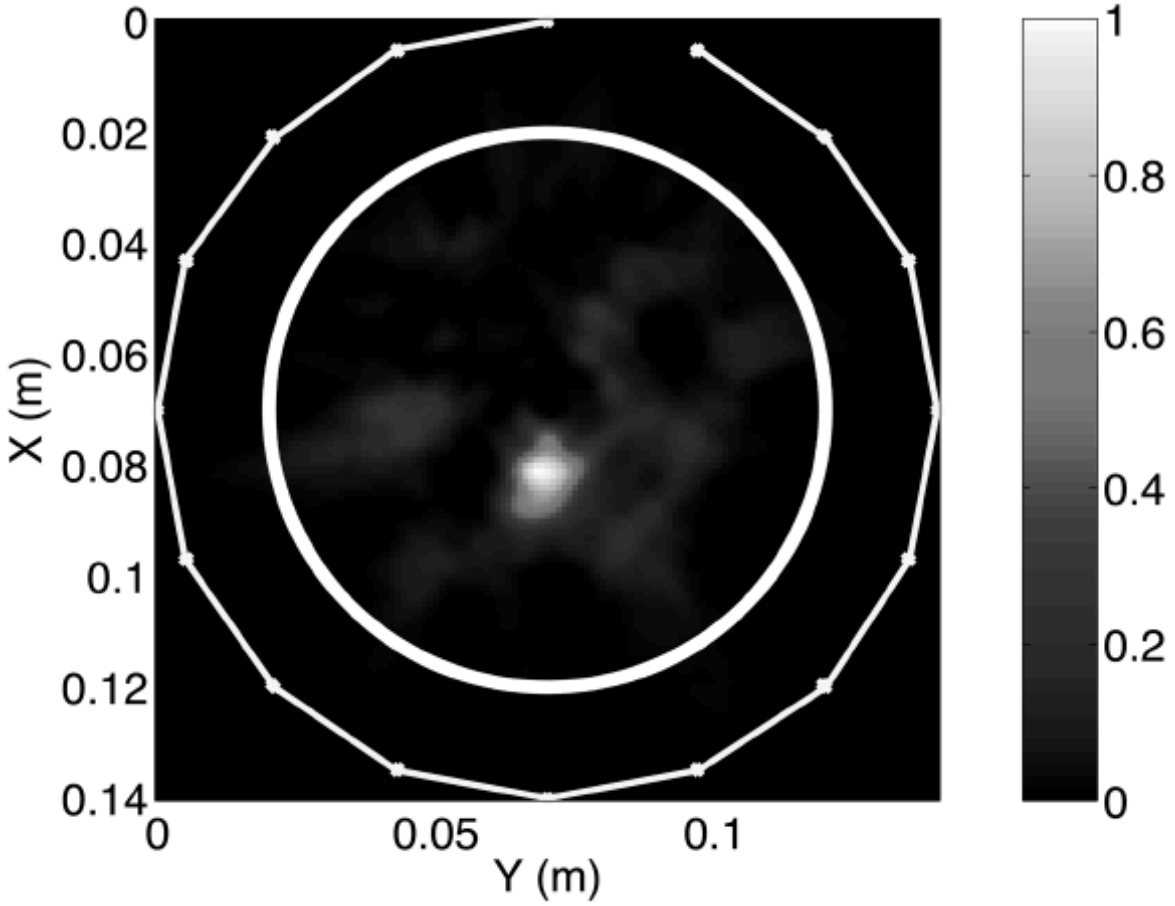

Figure 3: A typical TSAR Image – courtesy Dr. Elise Fear, University of Calgary

Our expertise is in seismic imaging, as in the following sample. The imaging goal is the same. However, the scale is different.

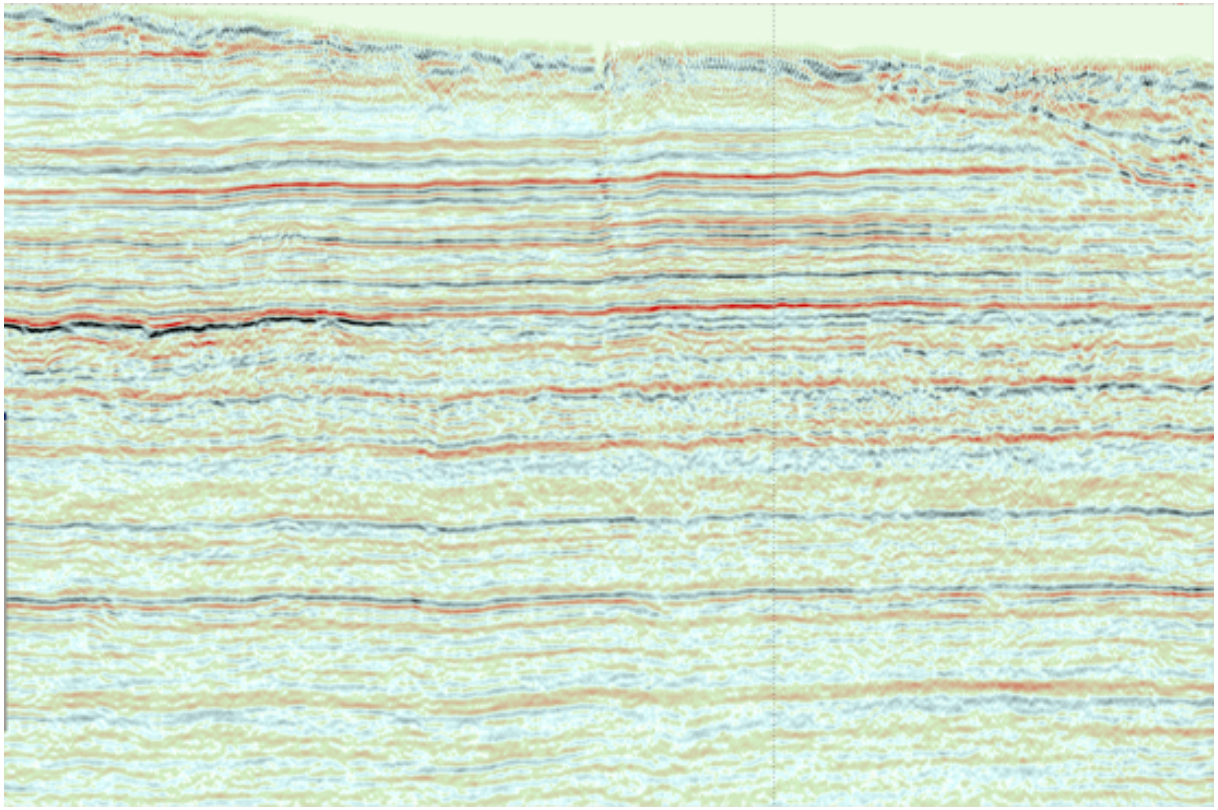

Figure 4: A cross section of the earth subsurface, 10 km by 5 km.

Our imaging techniques focus on numerically modelling the propagation of a wave (acoustic, seismic, microwave) through a medium of variable physical characteristics (density, elasticity, permeability, permittivity).

We use time-frequency methods, deconvolution, numerical wave propagators, and eventually inverse theory to produce the images.

Gabor transform

The Gabor transform is a short-time variant of the usual Fourier transform

$$(\mathcal{F}f)(\omega) = \int_{-\infty}^{\infty} f(s)e^{-2\pi is\omega}\,ds$$

obtained by localizing with a Gaussian window of fixed width, centred at time t,

$$(\mathcal{G}f)(t,\omega) = \int_{-\infty}^{\infty} f(s)e^{-(s-t)^2}e^{-2\pi is\omega}\,ds.$$

This is similar to the Stockwell transform, which uses variable width windows

$$(\mathcal{S}f)(t,\omega) = |\omega| \int_{-\infty}^{\infty} f(s)e^{-(s-t)^2\omega^2}e^{-2\pi is\omega}\,ds,$$

and is simply a phase-adjusted version of the usual continuous wavelet transform

$$(\mathcal{W}f)(t,a) = \left(\frac{1}{|a|}\right)^{1/2} \int_{-\infty}^{\infty} f(s)\phi(\frac{s-t}{a})\,ds,$$

where $a = 1/\omega$ is scale, and ϕ is the complex Morlet wavelet

$$\phi(s) = e^{-s^2} e^{-2\pi i s}.$$

Any one of the last three transforms gives a time-frequency representation of the signal f as a function of two variables (t, ω).

In our work, we find the Gabor transform to be the most useful representation in digital implementations.

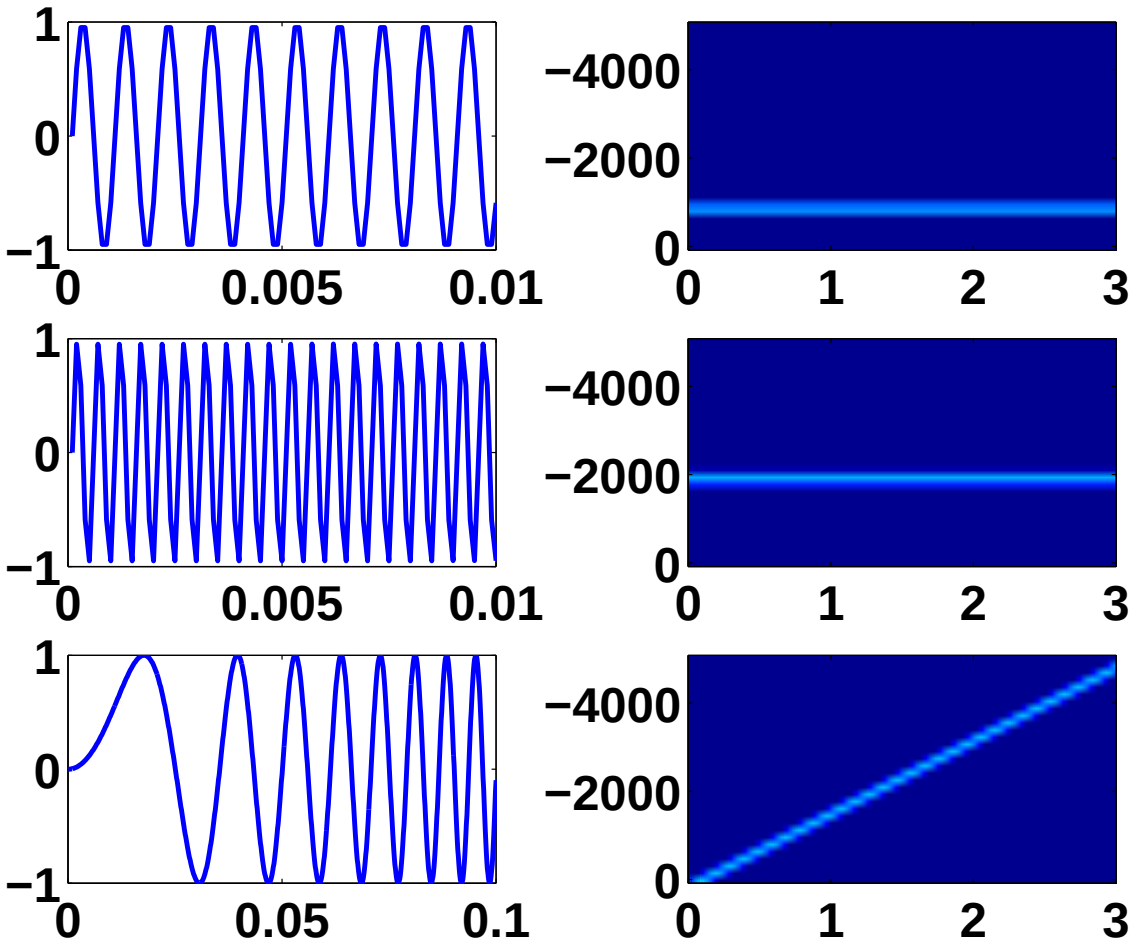

Figure 5: Gabor transforms of a 1kHz tone, a 2kHz tone, and a linear chirp.

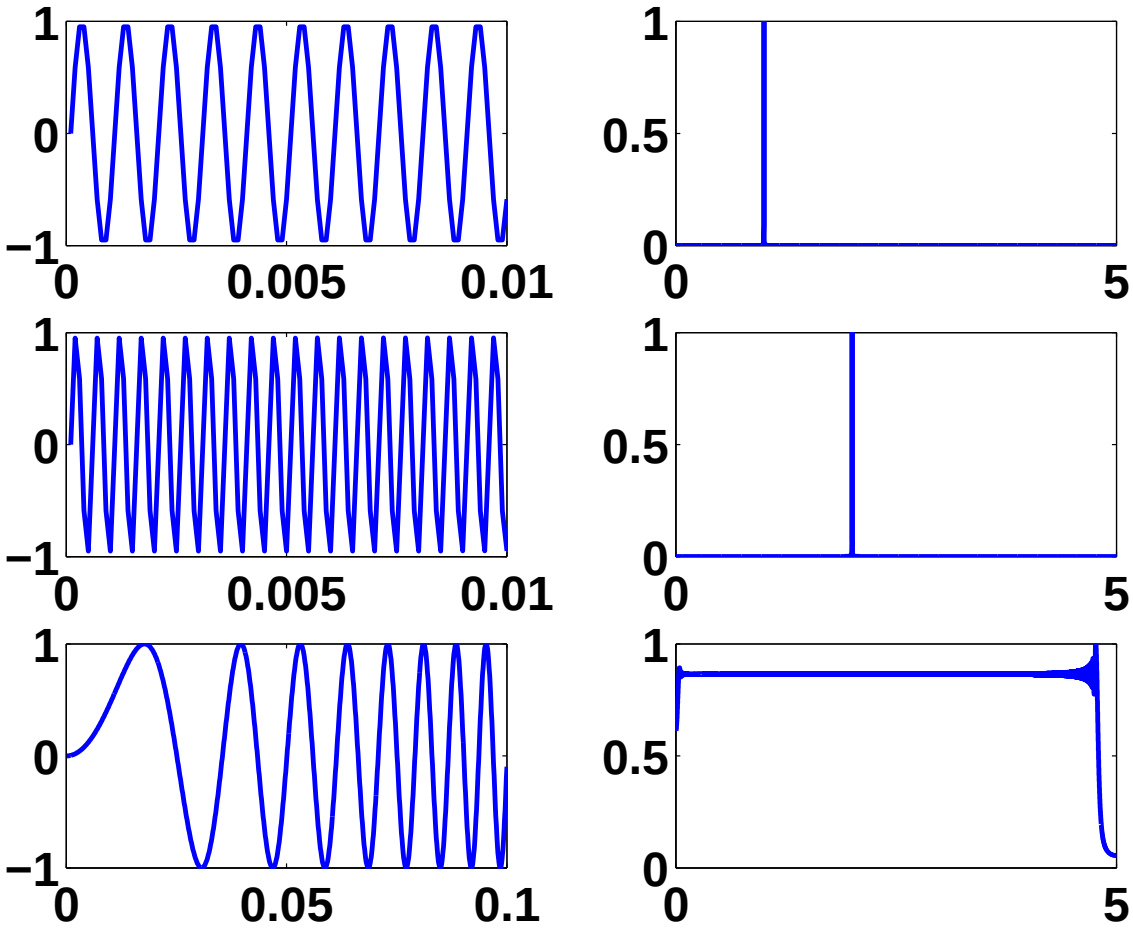

Figure 6: Contrast the info in FFT of a 1kHz tone, a 2kHz tone, and a linear chirp.

Conceptually, the Gabor transform is obtained by windowing the signal at various times, and plotting the FFT of each corresponding windowed result.

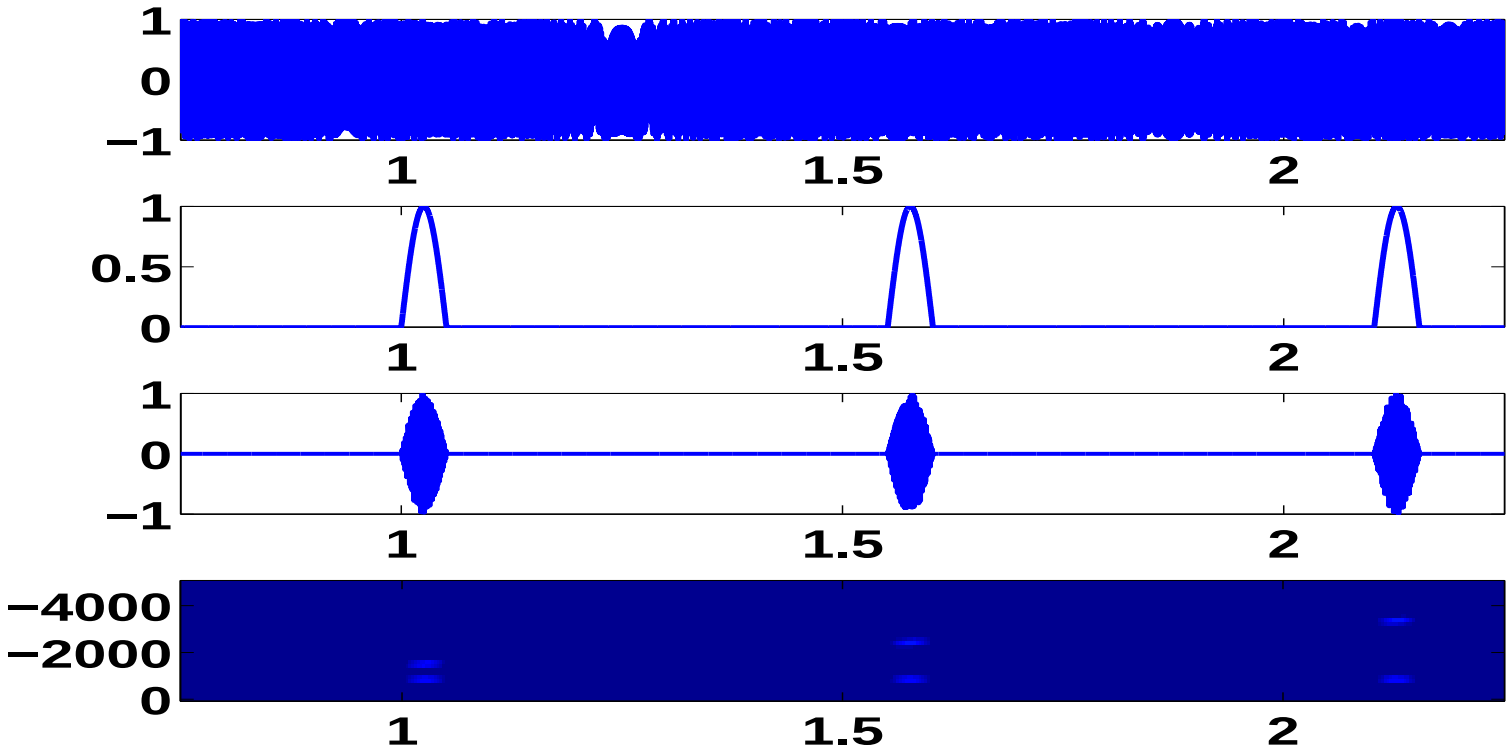

Figure 7: 1) Some signal. 2) Three windows. 3) Windowed signal. 4) FFTs.

Put these all together to obtain the full Gabor transform.

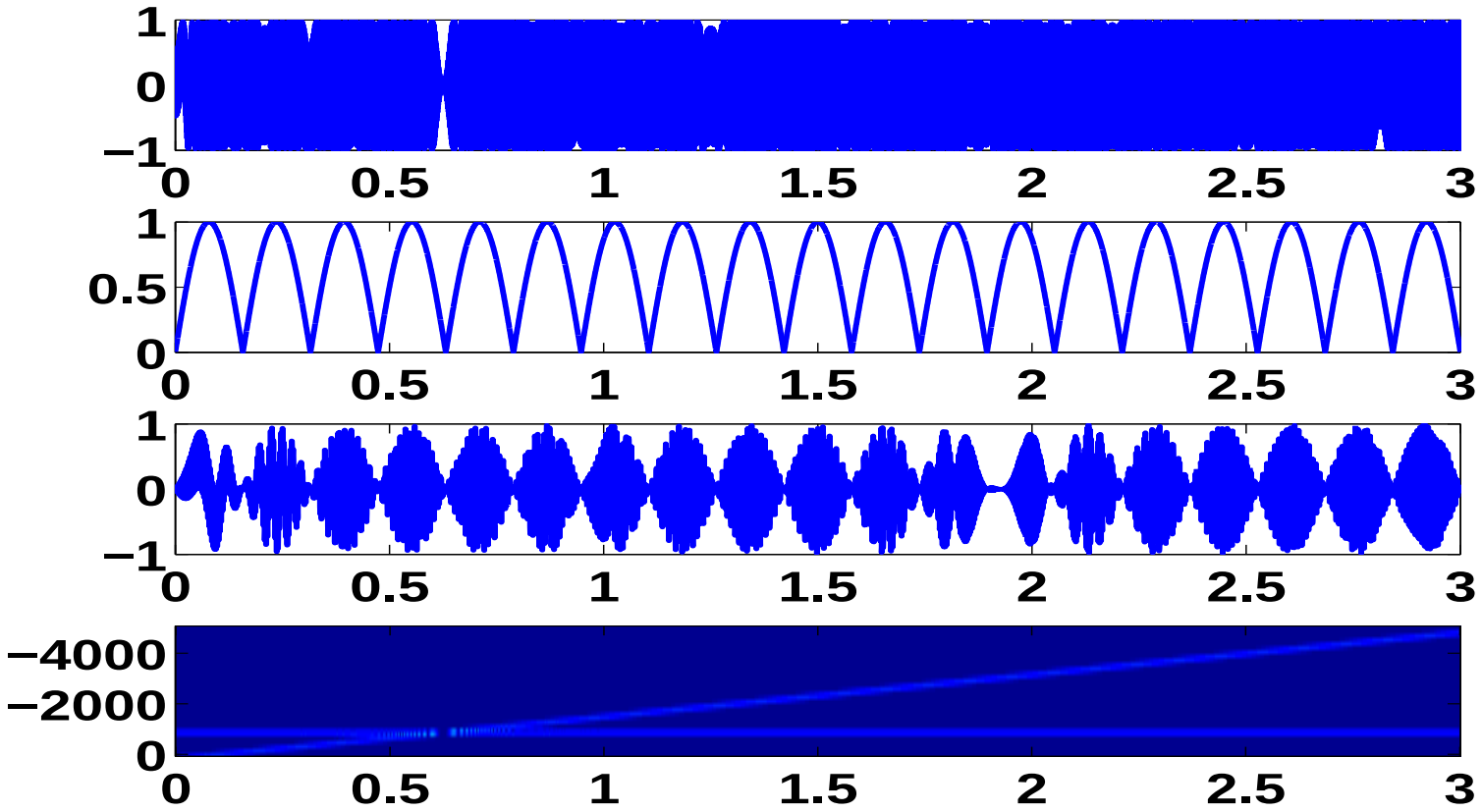

Figure 8: Building the full time-frequency representation.

Example: Vibroseis signal

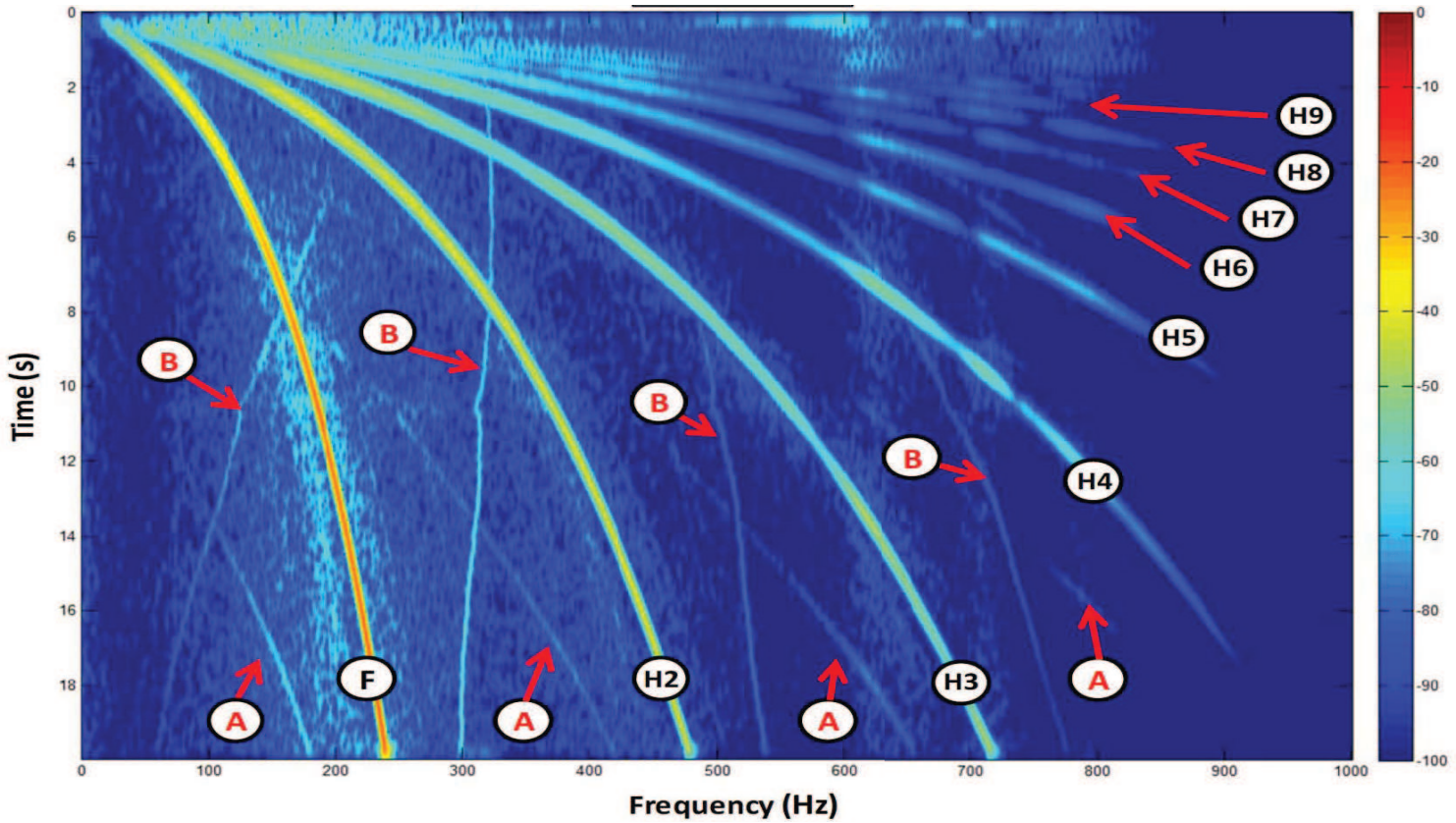

Figure 9: Rich detail in the time-frequency representation.

Example: the physical source

Figure 10: A Vibroseis truck, shaking the earth.

Gabor multipliers

Given a time-frequency representation of a signal

$$(\mathcal{G}f)(t,\omega),$$

it can be modified by multiplication with some function $a(t,\omega)$, to obtain

$$a(t,\omega)(\mathcal{G}f)(t,\omega) = (M_a\mathcal{G}f)(t,\omega),$$

where M_a is the multiplication operator. A new signal is obtained by pulling back to the time domain, using the adjoint of $\mathcal{G}$,

$$\tilde{f}(t) = (\mathcal{G}^* M_a \mathcal{G} f)(t).$$

The operator $G_a = \mathcal{G}^* M_a \mathcal{G}$ is called the Gabor multiplier with symbol a.

As a simple example, take $a(t,\omega) = 1$ in some region of interest, zero elsewhere.

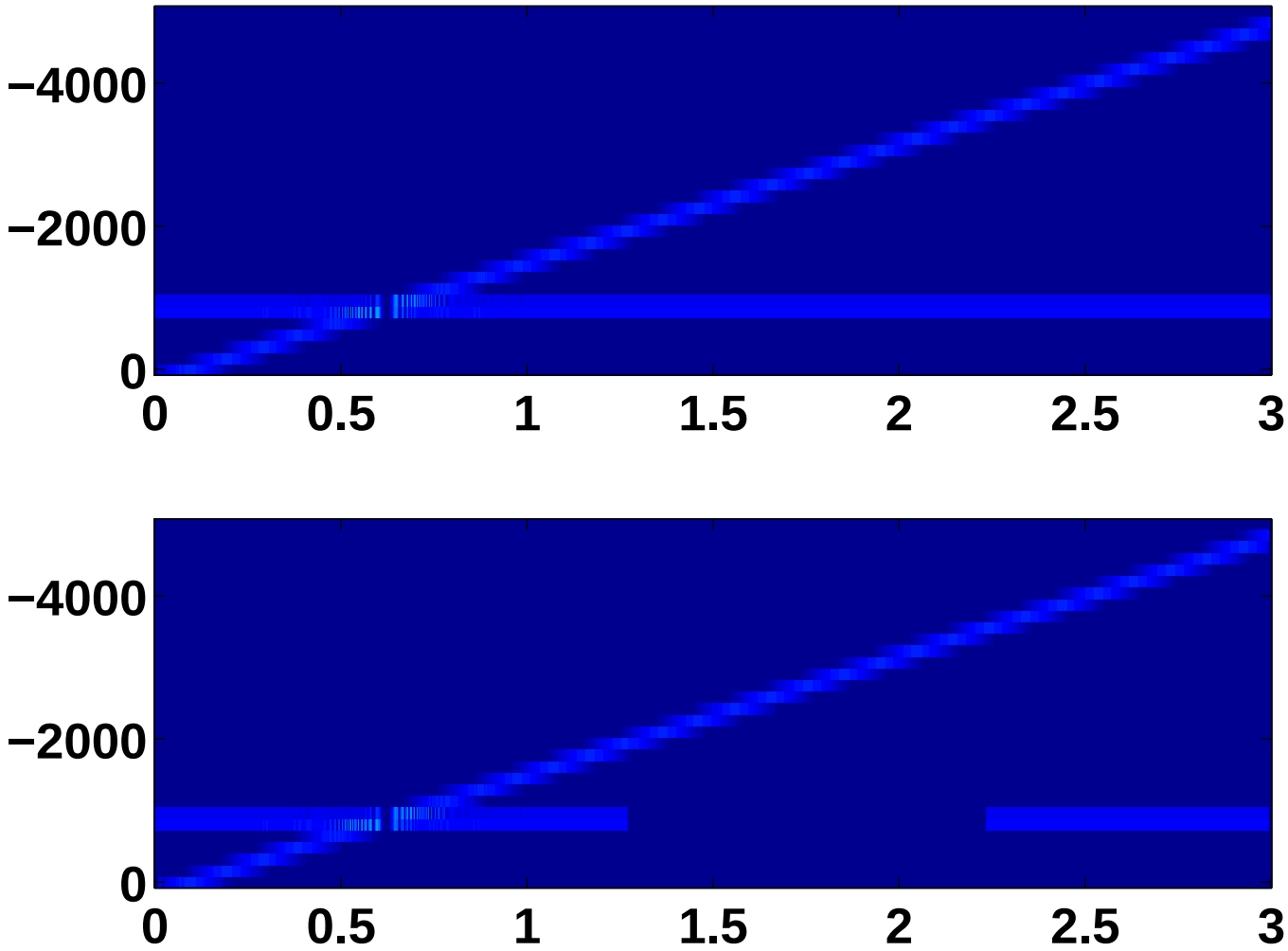

Figure 11: A beep+chirp signal, and a filtered version.

More generally, take any function for $a(t, \omega)$ to build a linear operator, which can be written as

$$(G_a f)(t) = \int_{-\infty}^{\infty} \int_{-\infty}^{\infty} a(s, \omega)(\mathcal{G} f)(s, \omega) e^{-(t-s)^2} e^{2\pi i t\omega} \, d\omega ds.$$

These Gabor multipliers are closely connected to pseudo differential operators K_σ defined as

$$(K_\sigma f)(t) = \int_{-\infty}^{\infty} \sigma(t, \omega)(\mathcal{F} f)(\omega) e^{2\pi i t\omega} \, d\omega.$$

There is a precise statement of the connection:

Theorem 1. [GLM] *The two operators G_a, K_σ are equal as linear operators on Swartz-class functions, if and only if*

$$e^{-(\pi^2\omega^2 + t^2)/2} (\mathcal{F} a)(\omega, t) = e^{-\pi i t\omega} (\mathcal{F}\sigma)(\omega, t)$$

as tempered distributions.

Note the Gaussian on the left, in the theorem. This indicates not all K_σ can be

represented by Gabor multipliers – only those with sufficiently fast decay in the Fourier domain. The precise formula shows the Kohn-Niremberg symbol σ is a smoothed version of the function a, with a phase correction.

The proof of the theorem involves a calculation of the integral kernel of both operators, as a distribution. The details depend on the choice of Gaussian windows in the Gabor transform; other choices of windows are possible.

In many applications, we often set $a = \sigma$ and hope for the best! That is, for $a = \sigma$, we trust that

$$G_a \approx K_\sigma.$$

There is some numerical and theoretical justification for this simplification.

Windows

The standard Gabor transform uses a Gaussian window, and is defined as

$$(\mathcal{G}f)(t,\omega) = \int_{-\infty}^{\infty} f(s)e^{-(s-t)^2}e^{-2\pi is\omega}\,ds.$$

The Gaussian can, in principle, be replaced by any reasonable function $g(t)$, and a variant of the Gabor transfer is defined as

$$(\mathcal{G}_g f)(t,\omega) = \int_{-\infty}^{\infty} f(s)g(s-t)e^{-2\pi is\omega}\,ds.$$

For this to work as a reasonable time-frequency representation, g should be concentrated near $t = 0$, and be smooth with few oscillations.

A different window $\gamma(t)$ could be used for the adjoint operator, and thus a general Gabor multiplier with symbol a, window g and dual window γ is defined as

$$G_a = G_{a,g,\gamma} = \mathcal{G}_\gamma^* M_a \mathcal{G}_g.$$

In many applications, we can choose g to be a compactly supported smooth function, and γ the constant function 1, or vice versa. With a technical assumption (compatibility), we restate the theorem connecting Gabor multipliers and pseudo differential operators.

Theorem 2. [GLM] *Given two compatible windows g, γ, the operators $G_{a,g,\gamma}, K_\sigma$ are equal as linear operators on Swartz-class functions, if and only if*

$$(\hat{\overline{g}} * \hat{\gamma}) \otimes (\overline{g} * \tilde{\gamma})(\mathcal{F}a) \ = |\langle g, \gamma \rangle|^2 e^{-2\pi i \varphi} (\mathcal{F}\sigma)$$

as tempered distributions, where φ is a phase function determined by g, γ.

The specifics of the theorem are spelled out in the following table, for a few interesting compatible window pairs.

Gabor vs. Kohn-Nirenberg symbols for compatible window pairs (g, γ)			
#	$g(t)$	$\gamma(\tau)$	Relation between $\mathcal{F}a(\eta, y)$ and $\mathcal{F}\sigma(\eta, y)$
1.	1	$\gamma \in \mathcal{S}_n$	$\frac{1}{\widehat{\overline{\gamma}}(0)}\widehat{\gamma}(\eta)\mathcal{F}a = \mathcal{F}\sigma$
2.	$e^{2\pi i\xi\cdot t}$	$\gamma \in \mathcal{S}_n$	$\frac{1}{\widehat{\overline{\gamma}}(-\xi)}\widehat{\gamma}(\eta+\xi)e^{-2\pi i\xi\cdot y}\mathcal{F}a = \mathcal{F}\sigma$
3.	e^{-mt^2}	$e^{-\mu\tau^2}$	$e^{-\frac{\pi^2}{m+\mu}\eta^2}e^{-\frac{m\mu}{m+\mu}y^2}\mathcal{F}a = e^{-\frac{2\pi m}{m+\mu}i\eta\cdot y}\mathcal{F}\sigma$
4.	$e^{t-e^{\alpha t}}$	$e^{\tau-e^{\alpha\tau}}$	$\frac{2^{2/\alpha}}{\Gamma(2/\alpha)}\Gamma\left(\frac{2}{\alpha}-\frac{2\pi i}{\alpha}\eta\right)\frac{e^y}{(1+e^{\alpha y})^{2/\alpha}}\mathcal{F}a = (1+e^{\alpha y})^{-\frac{2\pi i\eta}{\alpha}}\mathcal{F}\sigma$
5.	$e^{kt-e^{\alpha t}}$	$e^{\kappa\tau-e^{\alpha\tau}}$	$\frac{1}{\Gamma\left(\frac{k+\kappa}{\alpha}\right)}\Gamma\left(\frac{k+\kappa}{\alpha}-\frac{2\pi i}{\alpha}\eta\right)\left(\frac{e^{\frac{\kappa\alpha}{k+\kappa}y}+e^{-\frac{k\alpha}{k+\kappa}y}}{2}\right)^{-\frac{k+\kappa}{\alpha}}\mathcal{F}a = (1+e^{\alpha y})^{-\frac{2\pi i\eta}{\alpha}}\mathcal{F}\sigma$

Item 1 is the flat window solution, γ an arbitrary Swartz class function.

Item 3 is the general Gaussian case of various widths

Item 4, 5 is an interesting one-sided window, also compatible.

The one-sided window

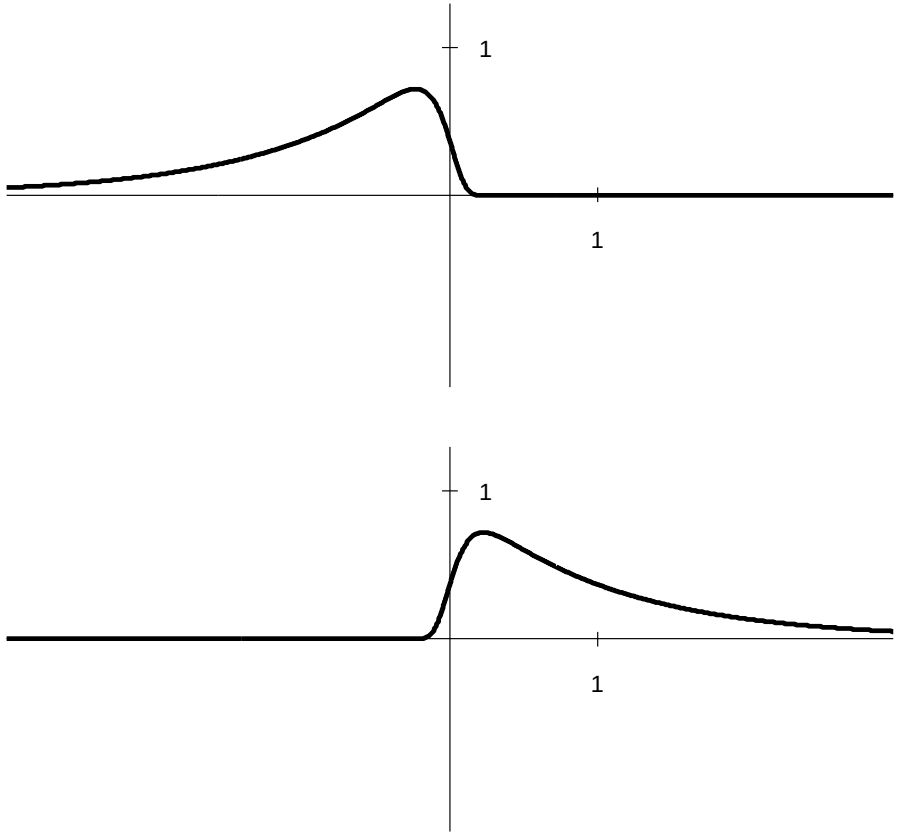

Figure 12: The double exponential $\exp(t - e^t)$ and its reverse.

Application - Gabor deconvolution

Gabor deconvolution is a non stationary extension of Wiener deconvolution. The basic model for a seismic wavelet $w(t)$ getting reflected off layers of the earth, represented by a time series $r(t)$, and recorded as data on the surface $d(t)$. The relation between the three functions is given by the convolution

$$d(t) = (w * r)(t) = \int_{-\infty}^{\infty} w(t-s)r(s)\,ds.$$

In the Fourier domain, the convolution becomes a multiplication, and we may write

$$\mathcal{F}d = (\mathcal{F}w)(\mathcal{F}r).$$

Both the reflectivity r and the wavelet w are unknown, but in practice there are ways to estimate the wavelet w. Thus we can recover reflectivity from the recorded data by computing the ratio

$$\mathcal{F}r = \frac{\mathcal{F}d}{\mathcal{F}w}.$$

This is basic idea of Wiener convolution.

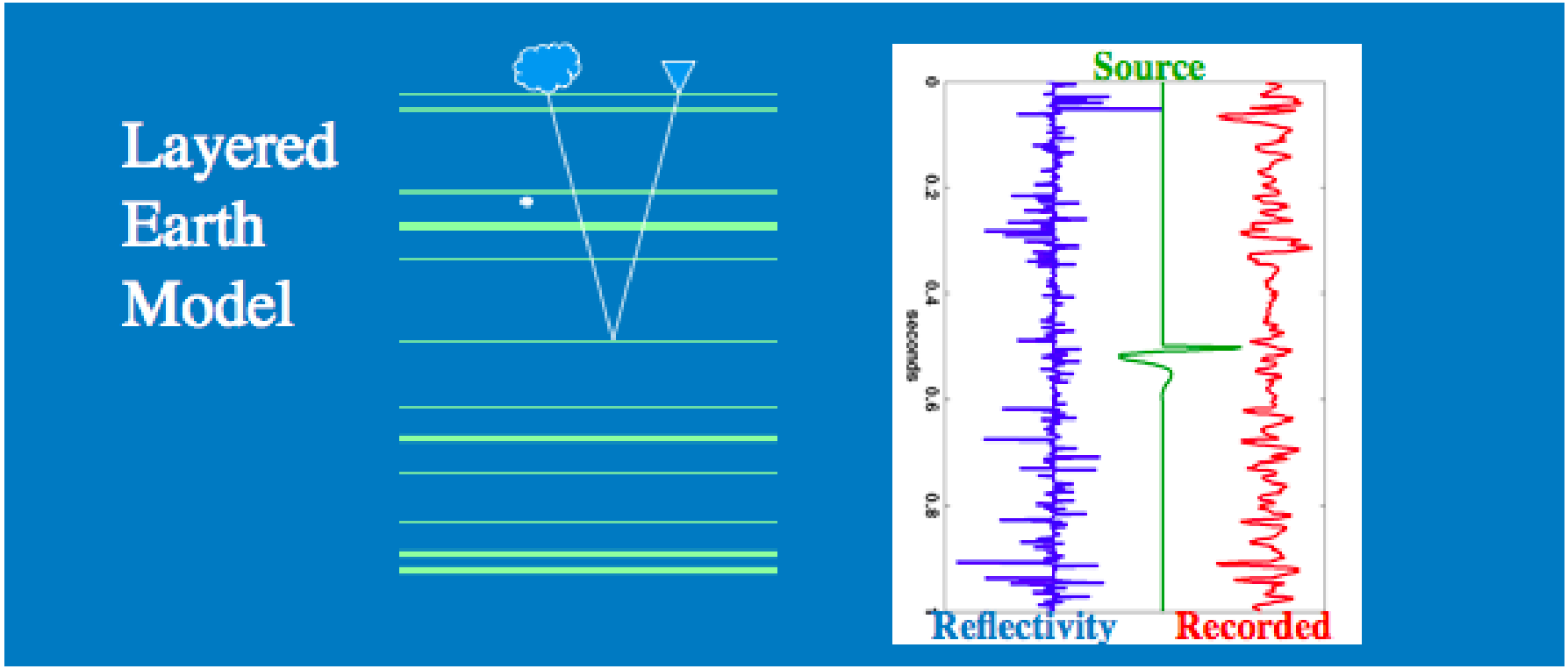

Figure 13: The 1D physical model for measuring reflectivity.

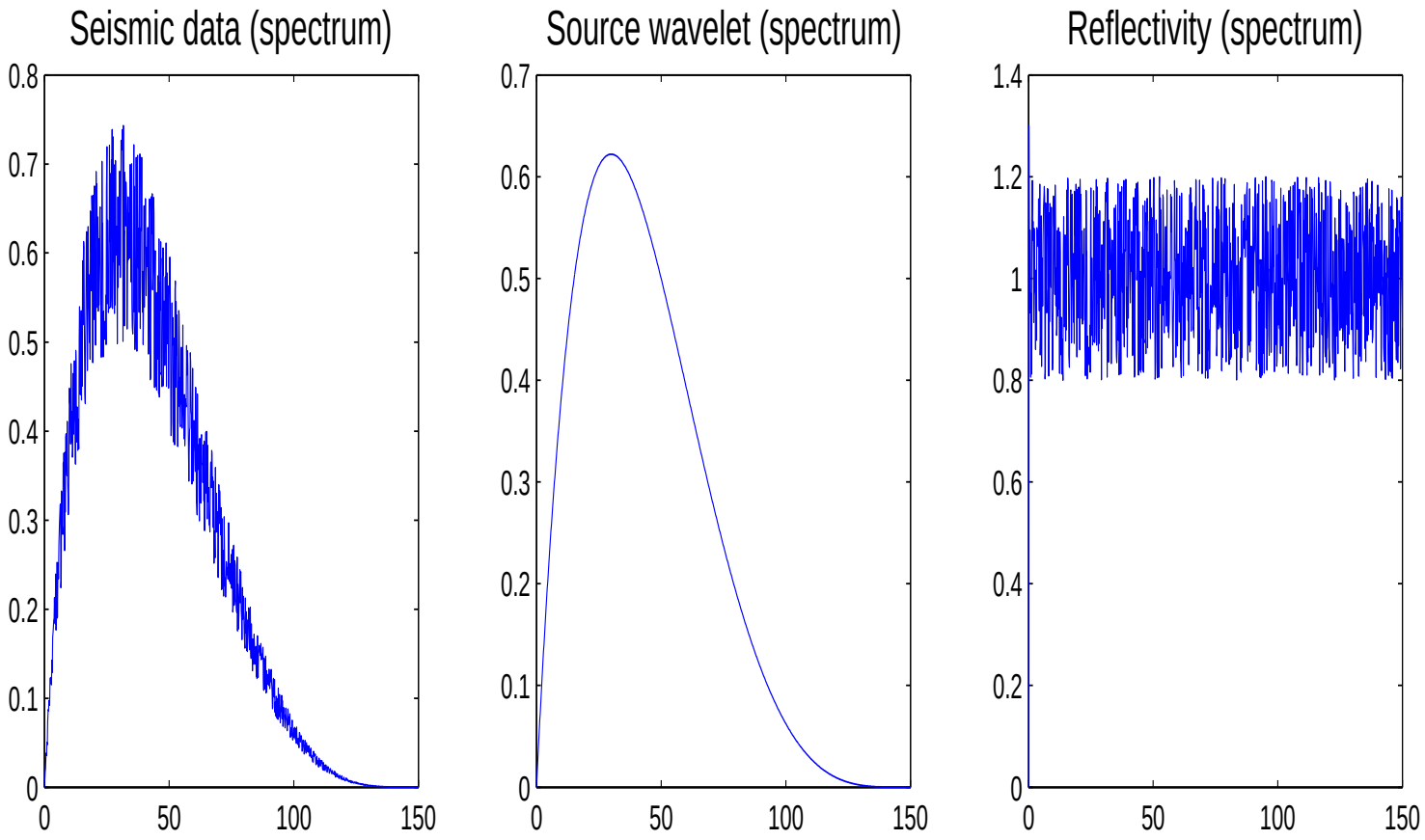

Figure 14: The Fourier transform of data, wavelet, reflectivity.

The key equation in Wiener decon

$$\mathcal{F}d = (\mathcal{F}w)(\mathcal{F}r)$$

is replaced by an analogous equality of Gabor transforms,

$$\mathcal{G}d = (\mathcal{G}w)M_a(\mathcal{G}r).$$

where the multiplier M_a has an exponentially decaying symbol

$$a(t,\omega) = e^{-\pi t\omega/Q} \times \text{ a phase factor}$$

which accounts for Q-attenuation in the earth.

Again, only the data $\mathcal{G}d$ is known. The wavelet factor $\mathcal{G}w$ is estimated, using a stationarity assumption

$$(\mathcal{G}w)(t,\omega) = \mathcal{F}w)(\omega),$$

while the multiplier factor $a(t,\omega)$ is estimated by assuming constant amplitude along hyperbolas.

This, plus some phase information, is enough to recover the Gabor transform of the reflectivity, as

$$\mathcal{G}r = \frac{\mathcal{G}d}{M_a \mathcal{G}w}.$$

Keep in mind, these are functions of two variables (t, ω).

The point of deconvolution is to remove the effects of the source wavelet and of the attenuation in the earth, leaving a sharper image of the reflectivity, or layers within the earth.

Gabor decon - examples

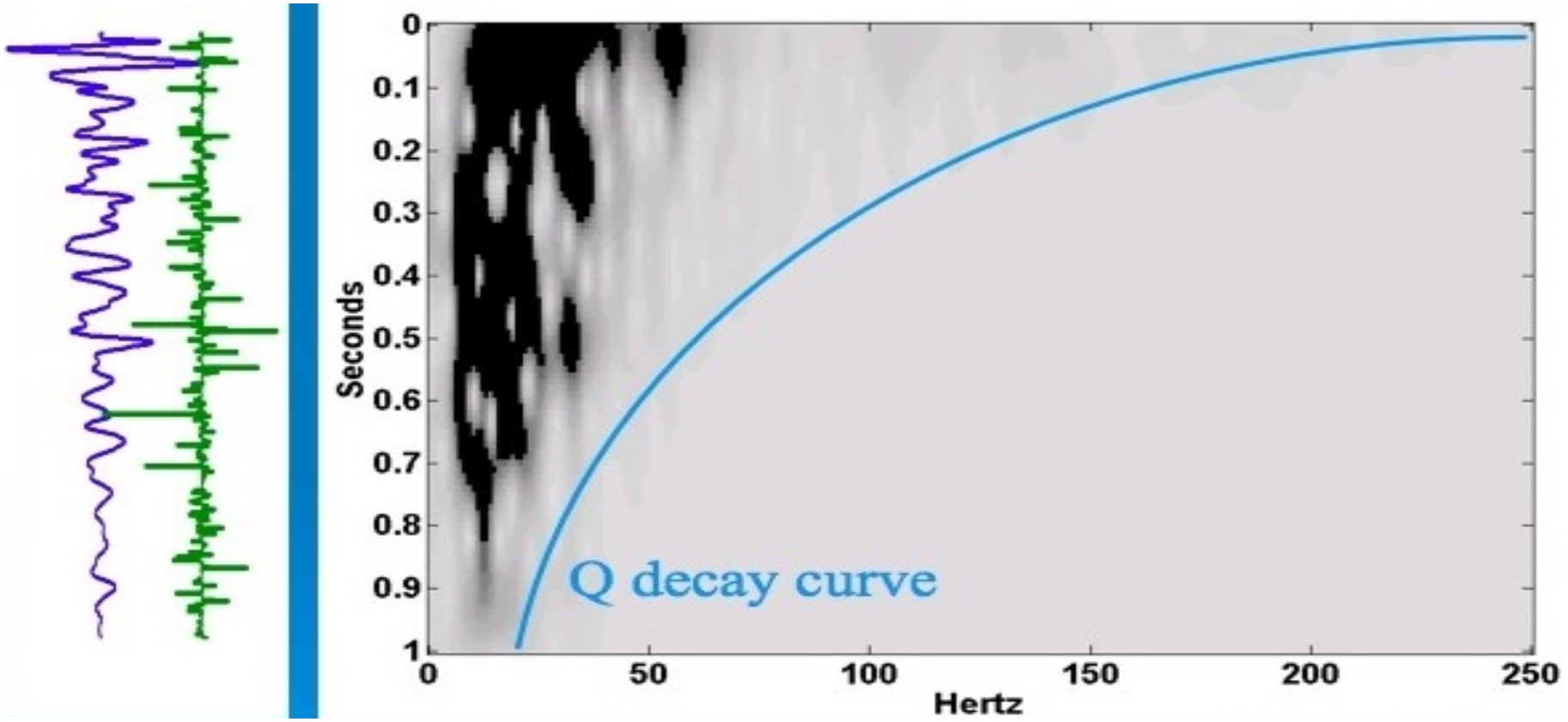

Figure 15: The recorded data, corresponding reflectivity, and Gabor transform.

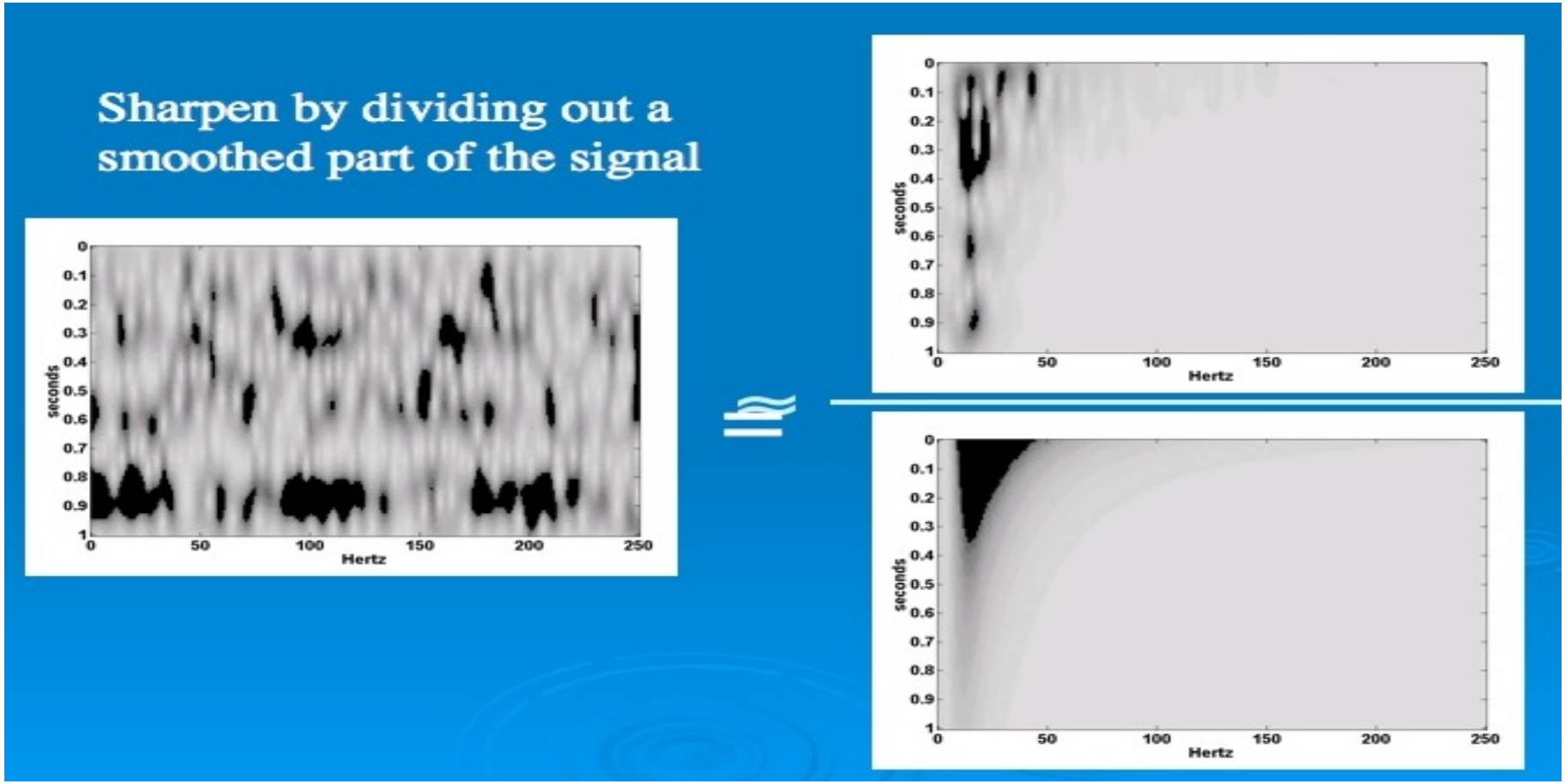

Figure 16: Estimating Gabor transform of reflectivity, as a ratio of two Gabors

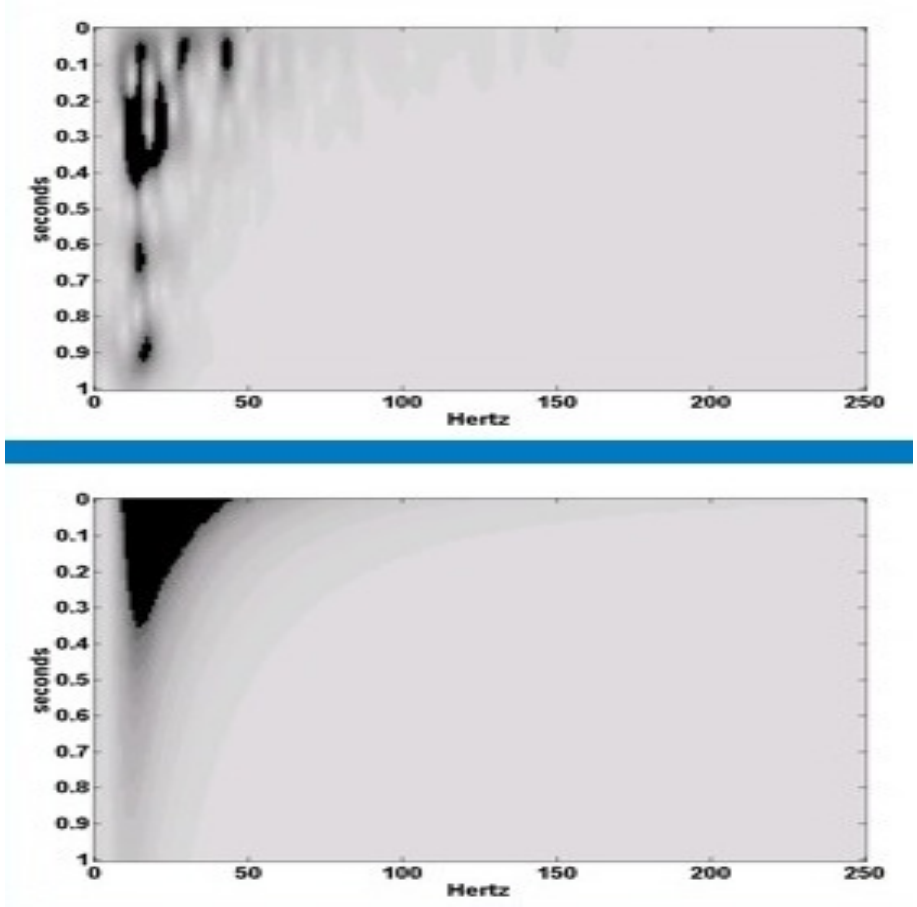

Figure 17: The denominator is a smoothed version of the numerator.

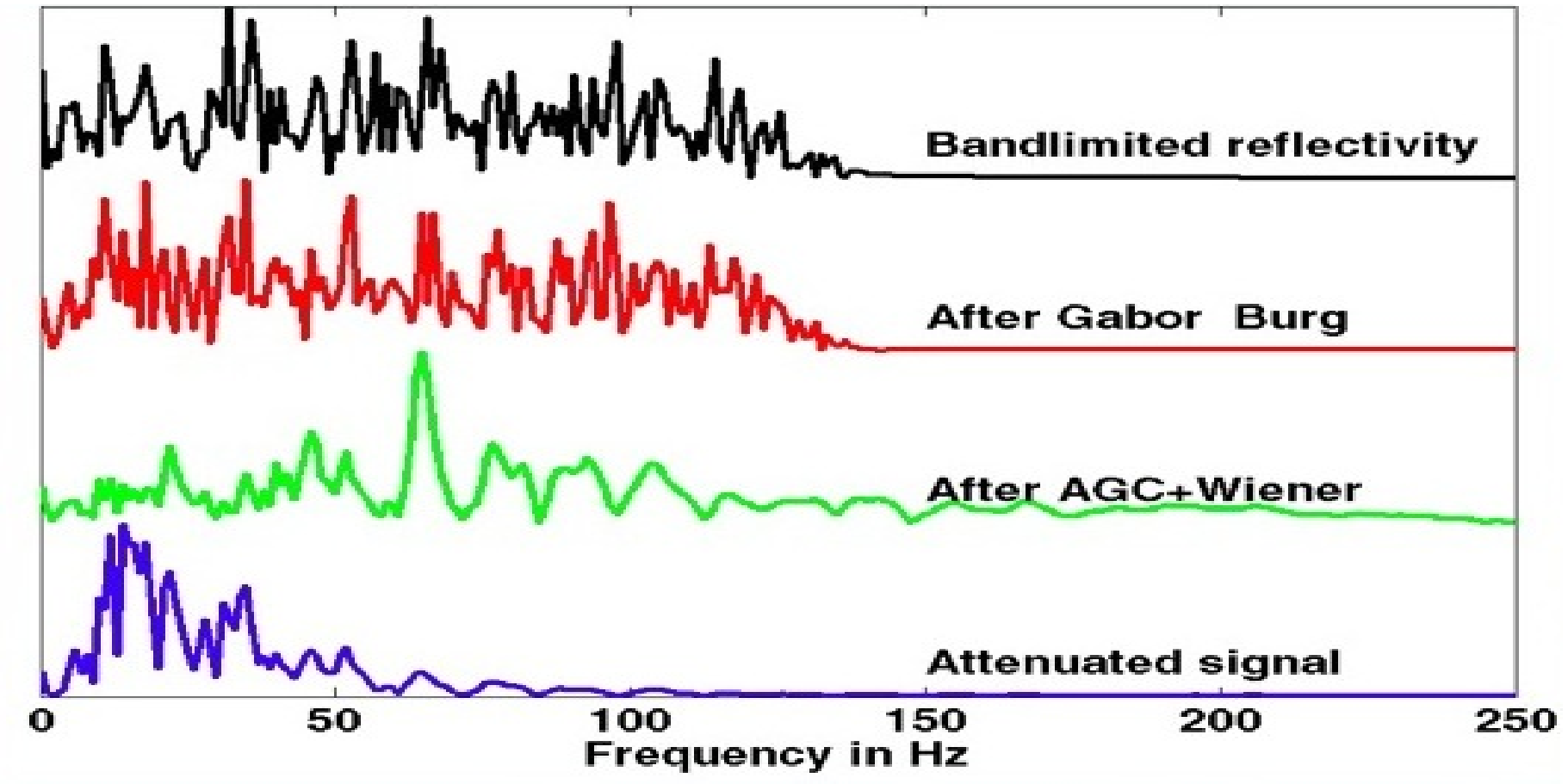

Figure 18: Results of Gabor decon on raw signal traces.

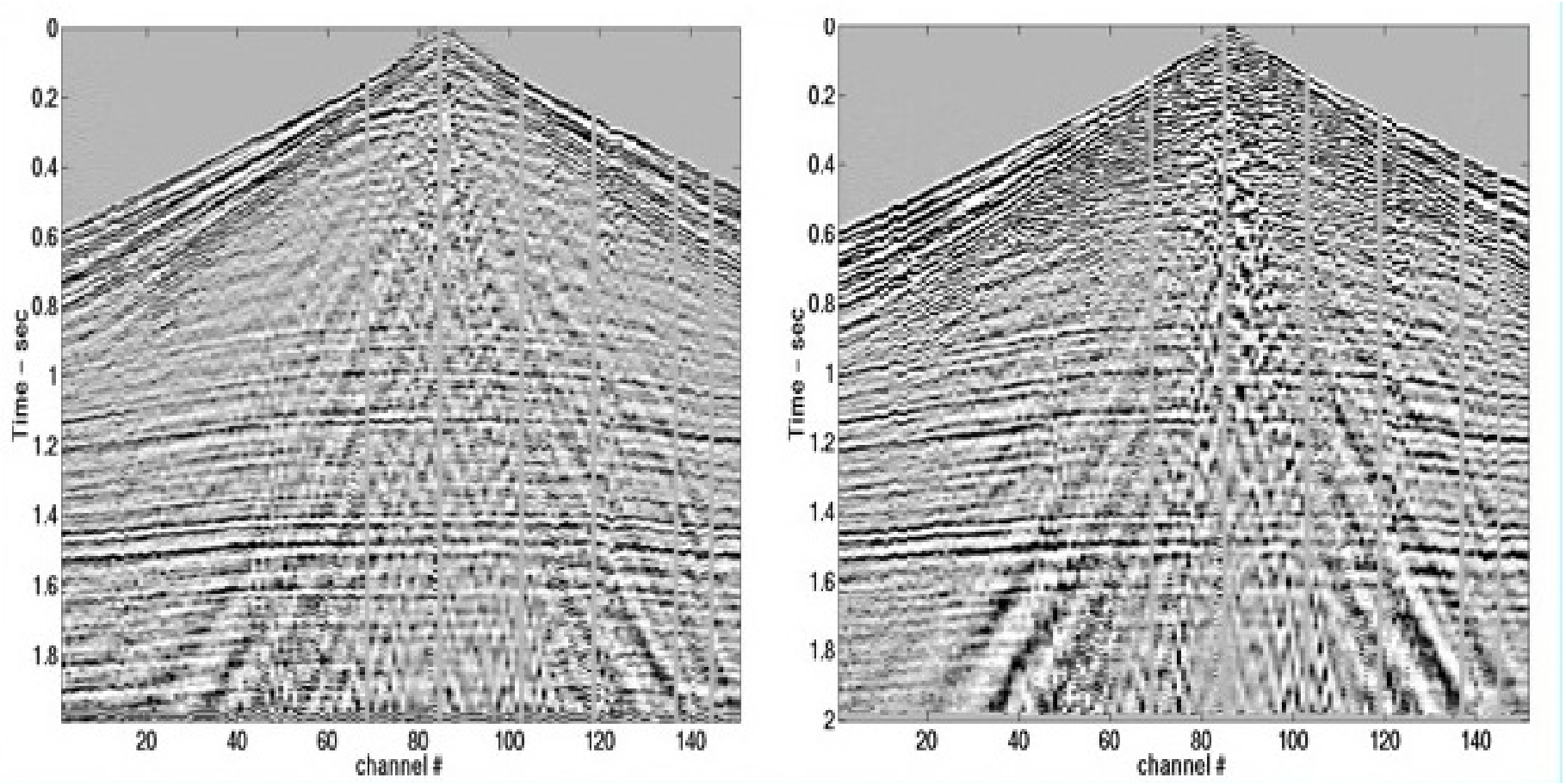

Figure 19: Gabor decon (left) and Wiener decon (right) on a single shot.

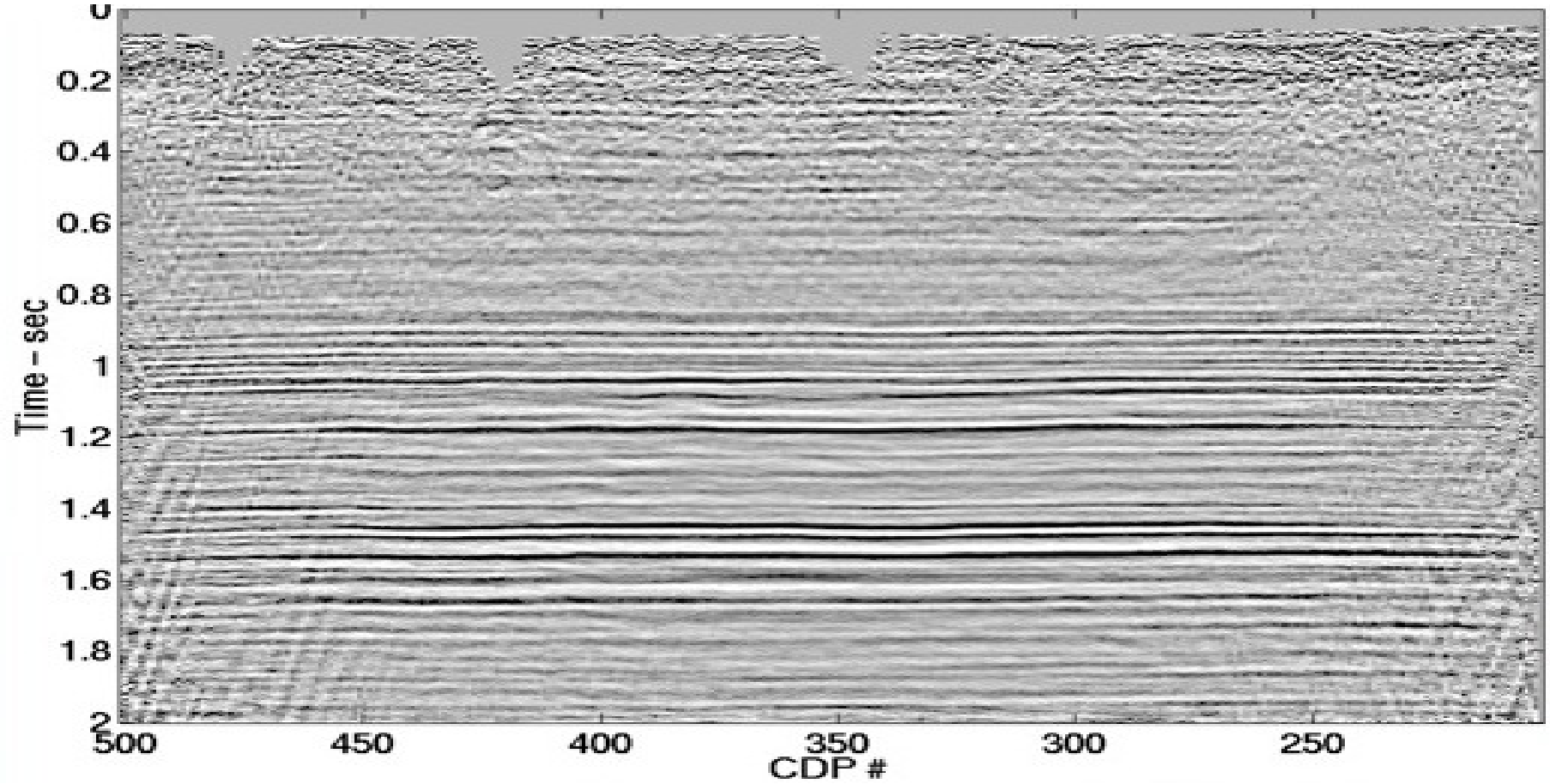

Figure 20: Wiener decon on stacked data, observe the horizontal features.

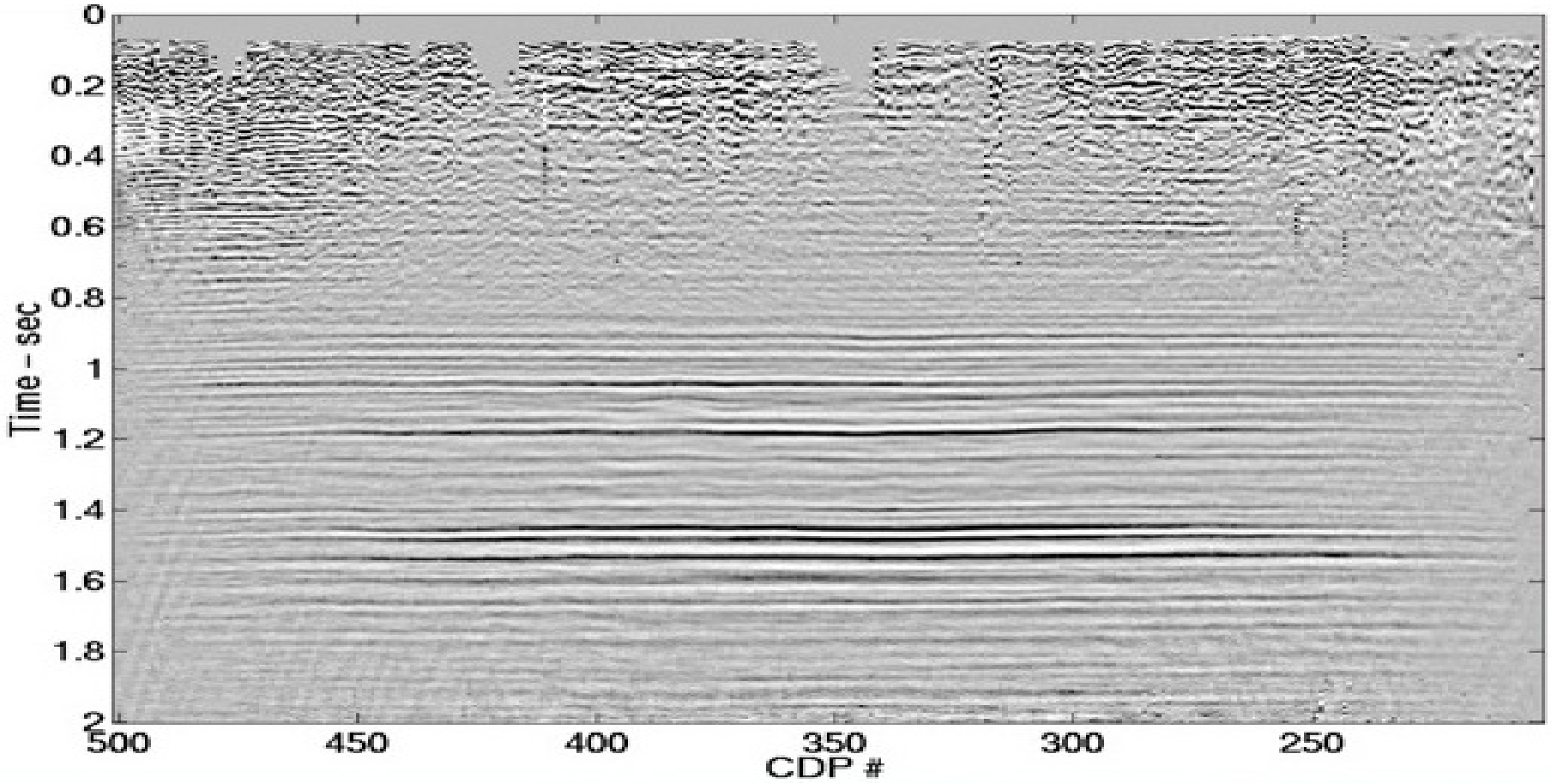

Figure 21: Standard Wiener decon on stacked data, for comparison.

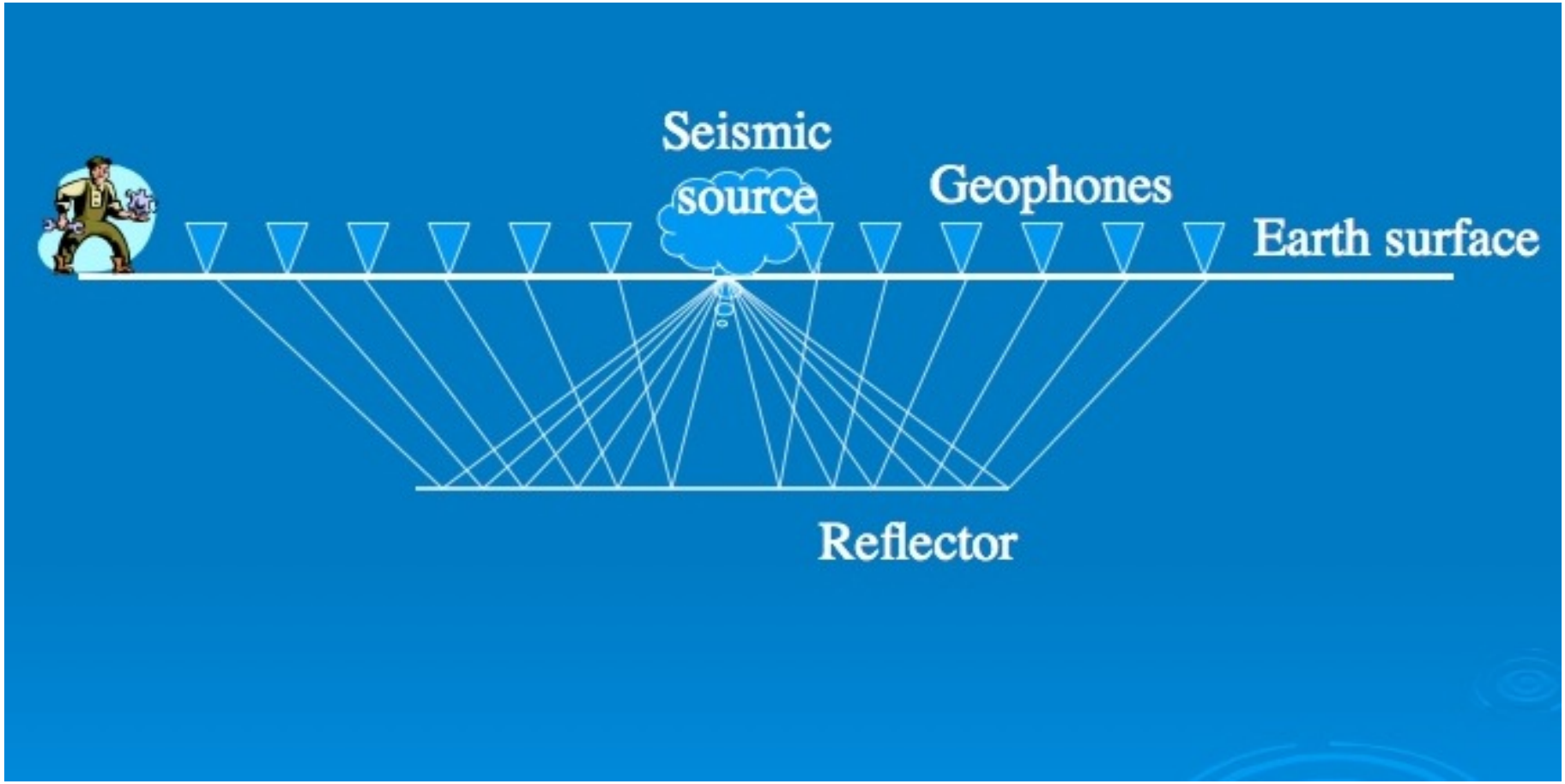

Figure 22: The standard seismic experiment – source on surface, reflector underground.

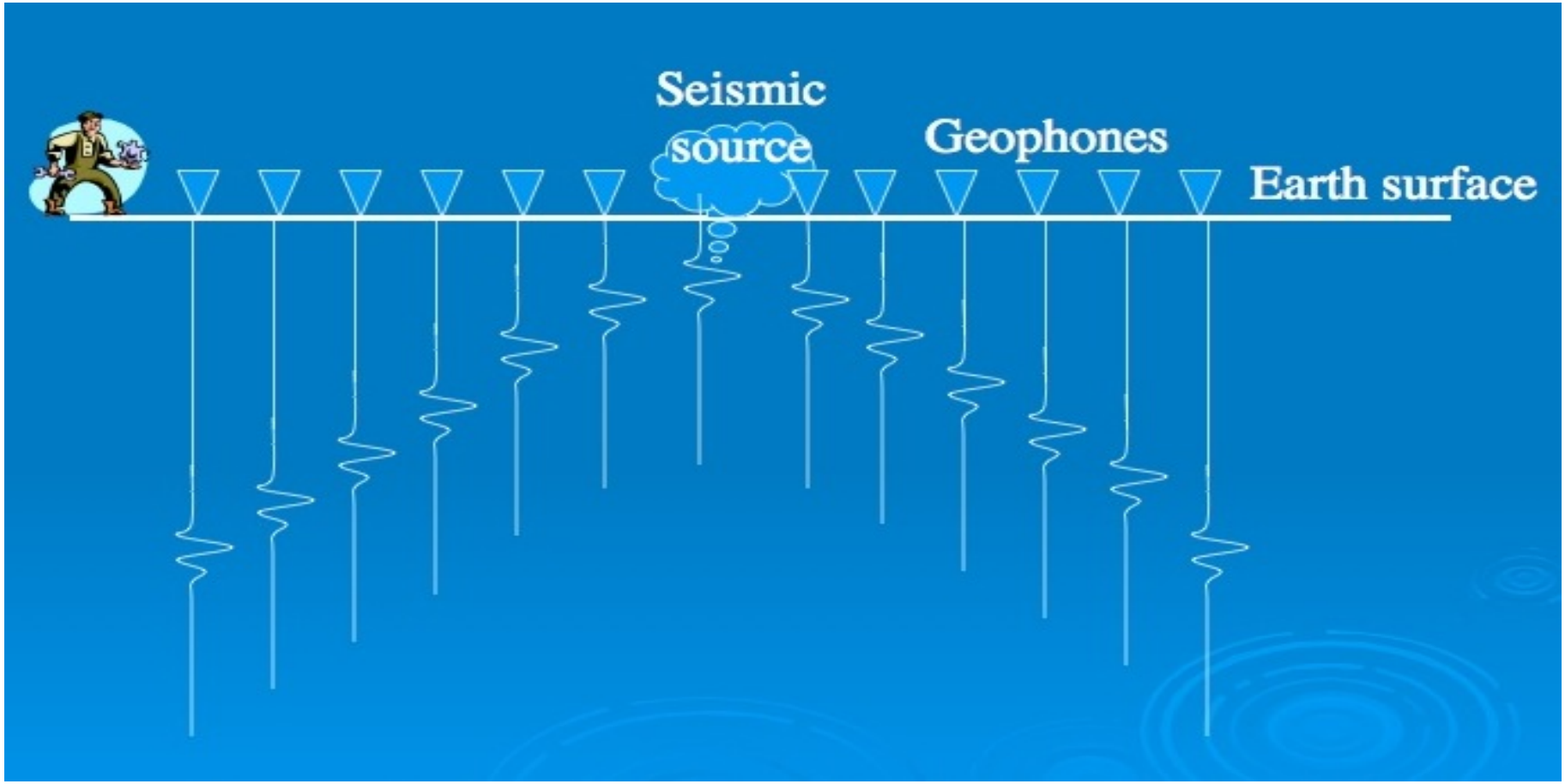

Figure 23: The reflections are recorded individually, form hyperbolas.

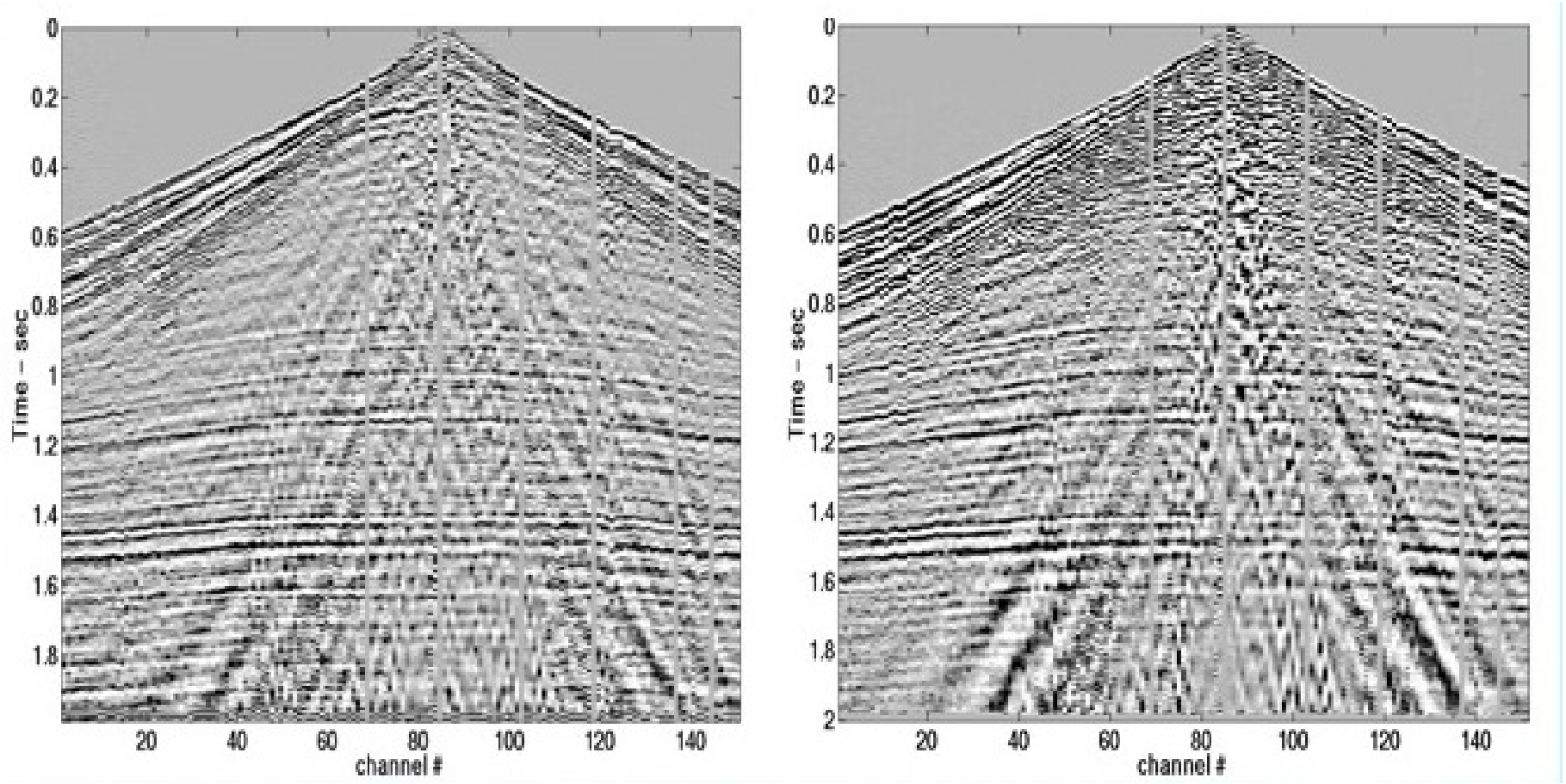

Figure 24: The horizontal hyperbolas represent the reflectors.

Example: the physical source

Figure 25: A dynamite source, shaking the earth.

Example: the physical source

Figure 26: A dynamite source, shaking the earth.

Gabor filtering in 2D - photos

The Gabor transform extends to higher dimensions, giving a transform of function in $\mathbb{R}^n$ to $\mathbb{R}^{2n}$.

$$(\mathcal{G}f)(\mathbf{x},\xi) = \int_{\mathbb{R}^n} f(\mathbf{y}) e^{-|\mathbf{x}-\mathbf{y}|^2} e^{-2\pi i \mathbf{y}\cdot\xi}\, d\xi,$$

with $\mathbf{x}, \mathbf{y}, \xi \in \mathbb{R}^n$.

A Gabor multiplier is constructed from a symbol $a = a(\mathbf{x}, \xi)$ using the adjoint formula

$$G_a = \mathcal{G}^* M_a \mathcal{G}.$$

In 2D, these give useful techniques for image procession, to create non-stationary (or localized) filter methods.

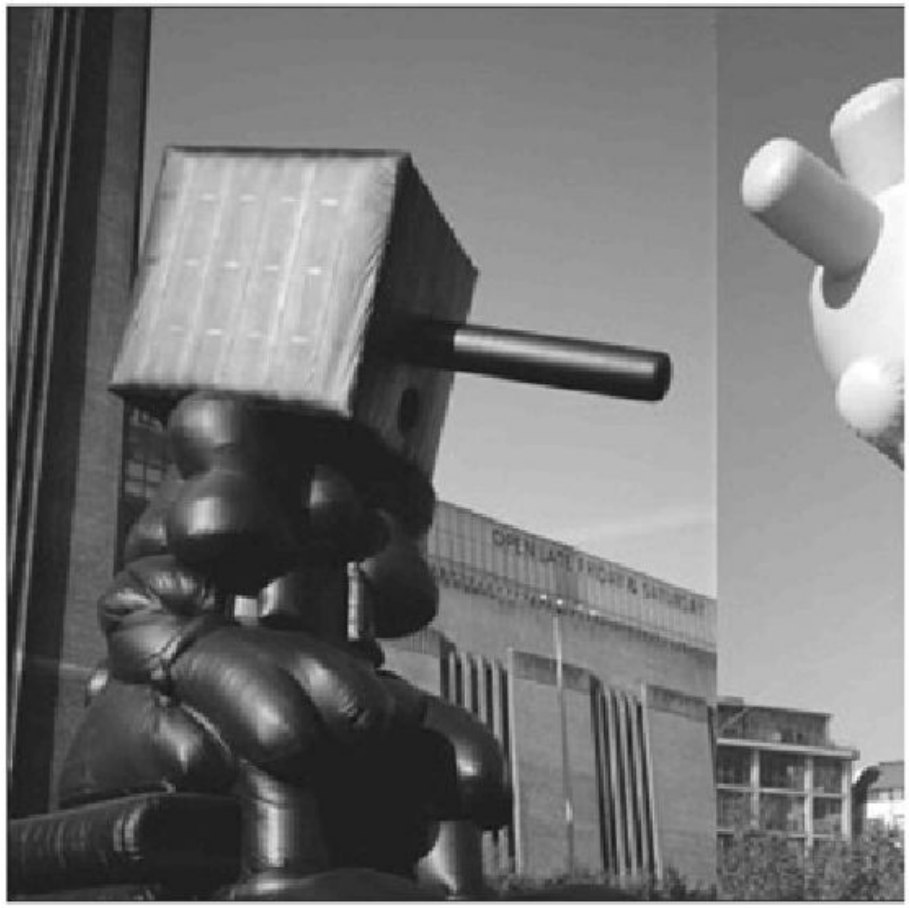

Figure 27: A 2D image, to process with a 2D Gabor multiplier.

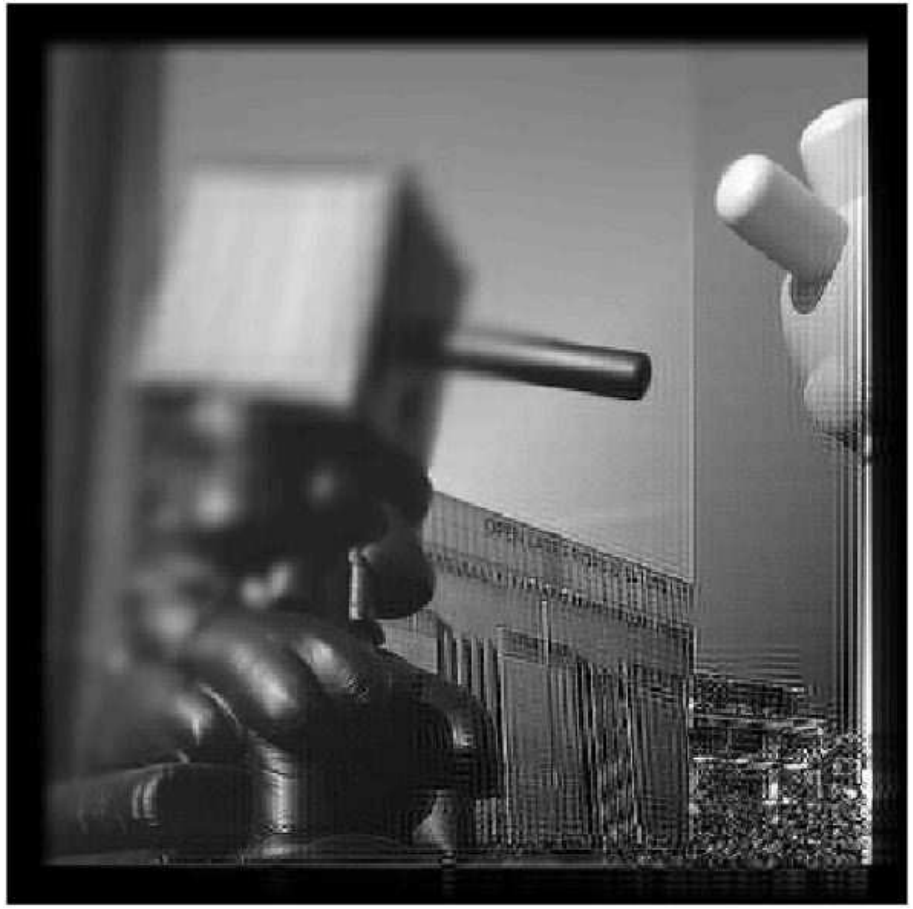

Figure 28: Non-stationary filtering. Top-left is blurred, bottom right sharpened.

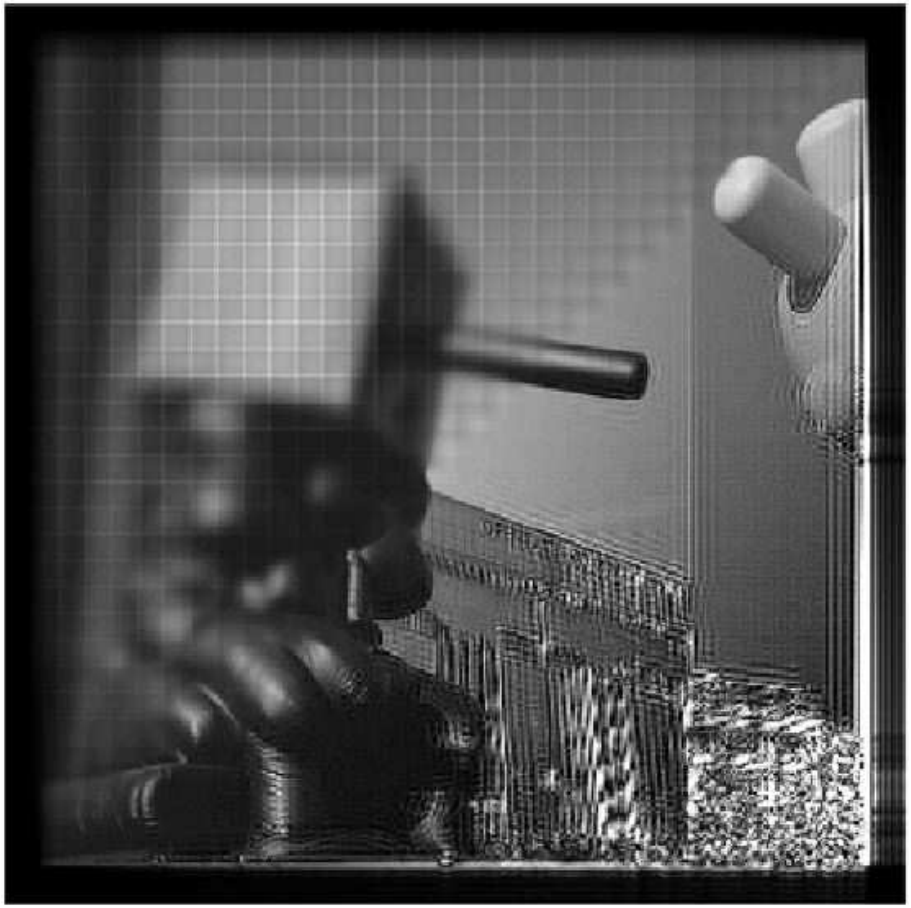

Figure 29: The windows form a discrete set. This buggy image shows the effect of poorly selected windows.

Gabor methods for imaging - part 2

Michael P.Lamoureux
University of Calgary

.

Joint work with P. Gibson, G. Margrave

.

Fields Workshop on Microlocal Methods in Medical Imaging

.

August 13–17, 2012

Doing math in Alberta

Figure 30: Out on a seismic data shoot, near an oil well.

Why the interest in Gabor multipliers?

We approximate solutions to linear PDEs with pseudodifferential operators:

$$(K_\sigma f)(t) = \int_{\mathbb{R}} \sigma(t,\omega)(\mathcal{F}f)(\omega)e^{2\pi i\cdot\omega}\, d\omega.$$

Computationally, this is too slow.

Typically, we take N samples in the t-variable, $t_1, t_2, \ldots, t_N$, another N samples in the ω-variable, so the integral (sum) requires $O(N^2)$ operation.

A good Gabor multiplier is about $O(N \log N)$.

In seismic, $N =$ a billion is common (3D grid, 1000x1000x1000):

– N FLOPS takes about one second

– $N \log N$ FLOPS takes about 30 seconds

– N^2 FLOPS takes 32 years.

Discrete Gabor transforms

Recall the Gabor transform was defined as a windowed Fourier Transform

$$(\mathcal{G}f)(t,\omega) = \int_{-\infty}^{\infty} f(s)w(s-t)e^{-2\pi is\omega}\,ds,$$

with a translates of a fixed window $w = w(s-t)$, often a Gaussian.

It is not necessary to use only one window; a discrete collection of functions

$$w_1, w_2, w_3, \ldots$$

can be used obtain a discrete formulation of the Gabor transform, with

$$(\mathcal{G}f)(t_k,\omega) = \int_{-\infty}^{\infty} f(s)w_k(s)e^{-2\pi is\omega}\,ds,$$

where the times t_k indicate the centres of the support of each window w_k.

As an example, here is a single window and the resulting localized signal.

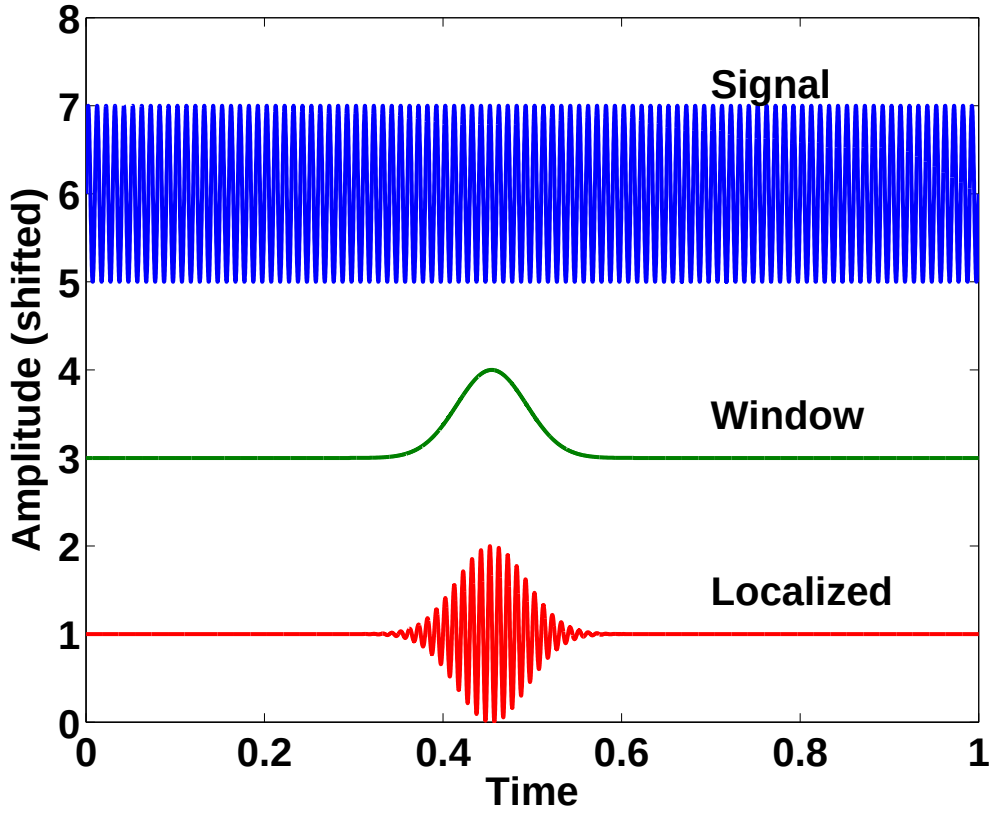

Figure 31: A single window, localizing the signal.

Take a discrete set of windows, to get a series of localizations

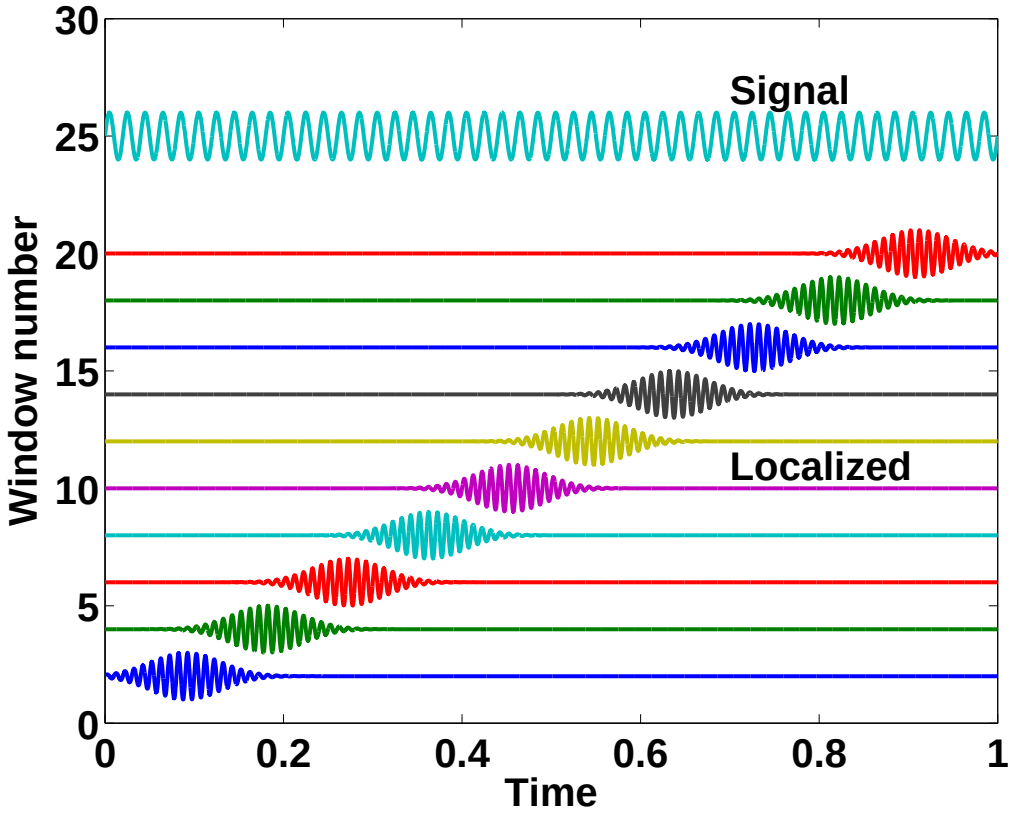

Figure 32: A set of 10 distinct windows.

The windows could even be of different shapes, boxcars, or smooth splines

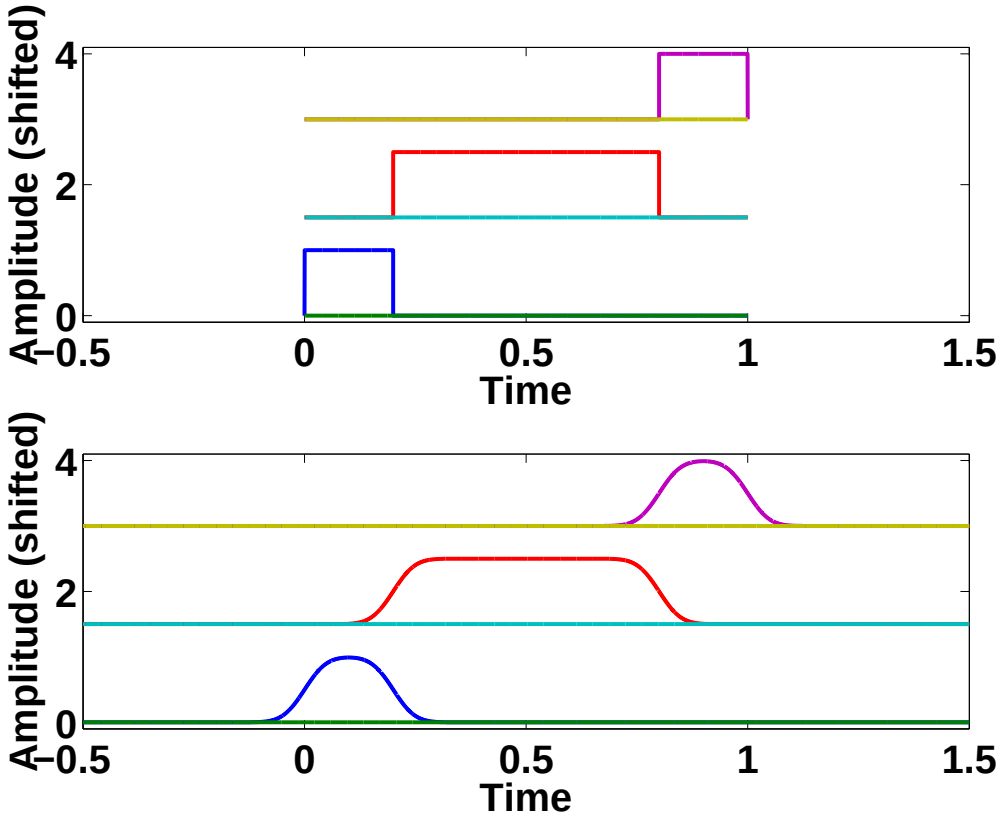

Figure 33: Three boxcar windows, and three splines.

A 2D example. One could use a regular pattern of shifted 2D gaussians:

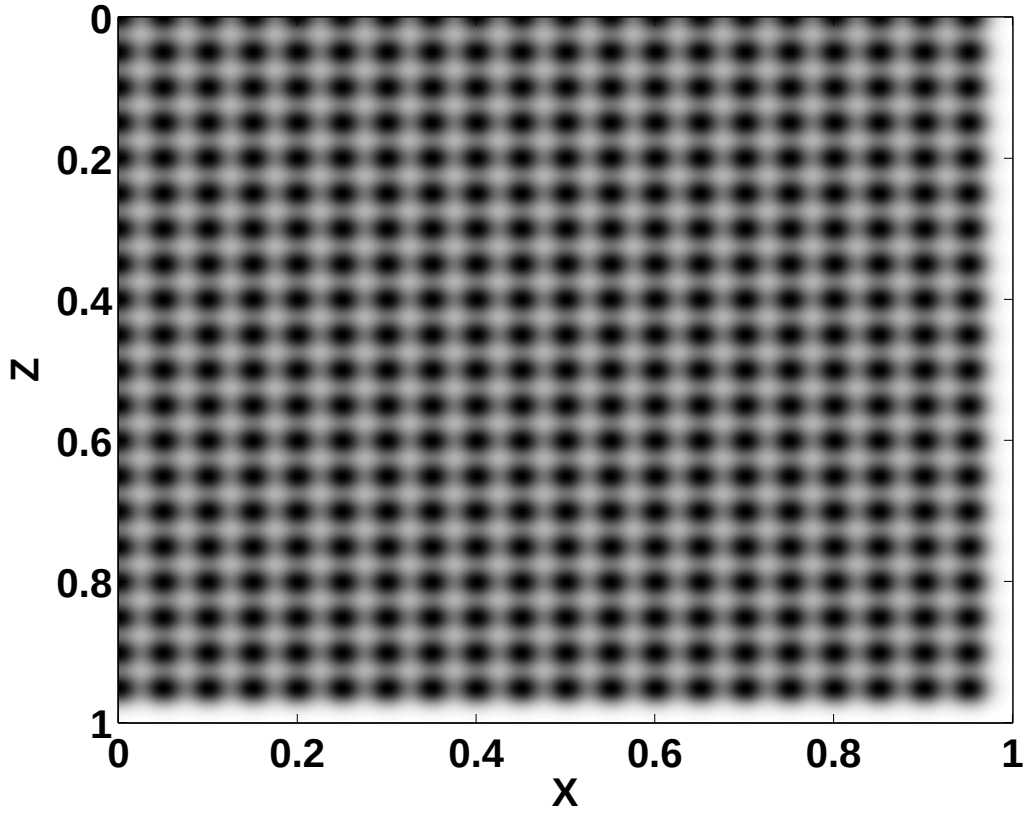

Figure 34: Regular tiling of plane by windows.

Or, in 2D, use windows with supports in unusual shapes like this.

,

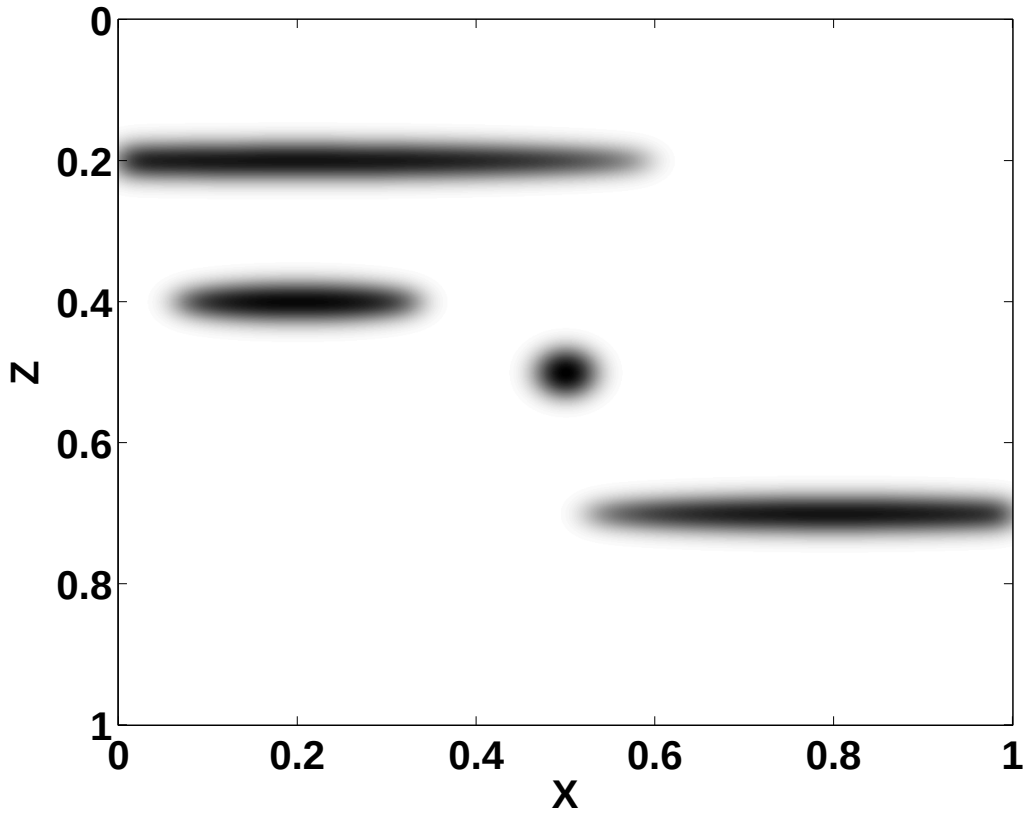

Figure 35: Non-regular window supports.

This would be useful for a velocity field following layers in the solid ilike this:

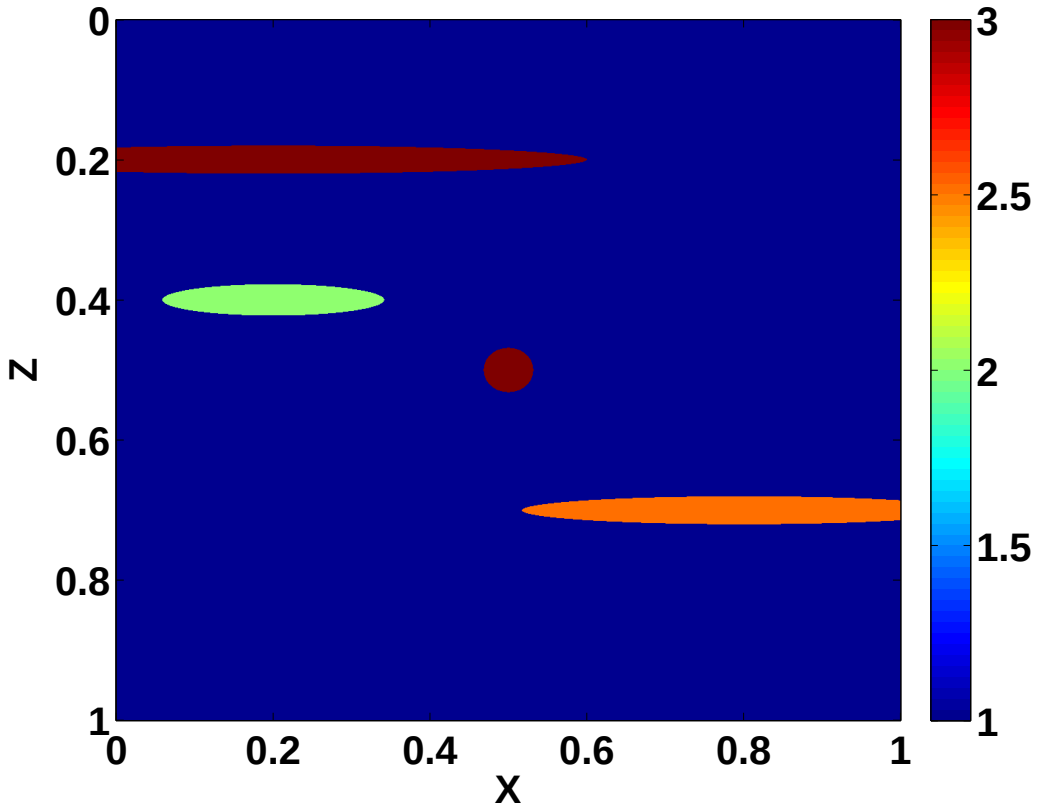

Figure 36: A complex velocity model, in layers.

In a complex medium, we model with a few, irregular windows

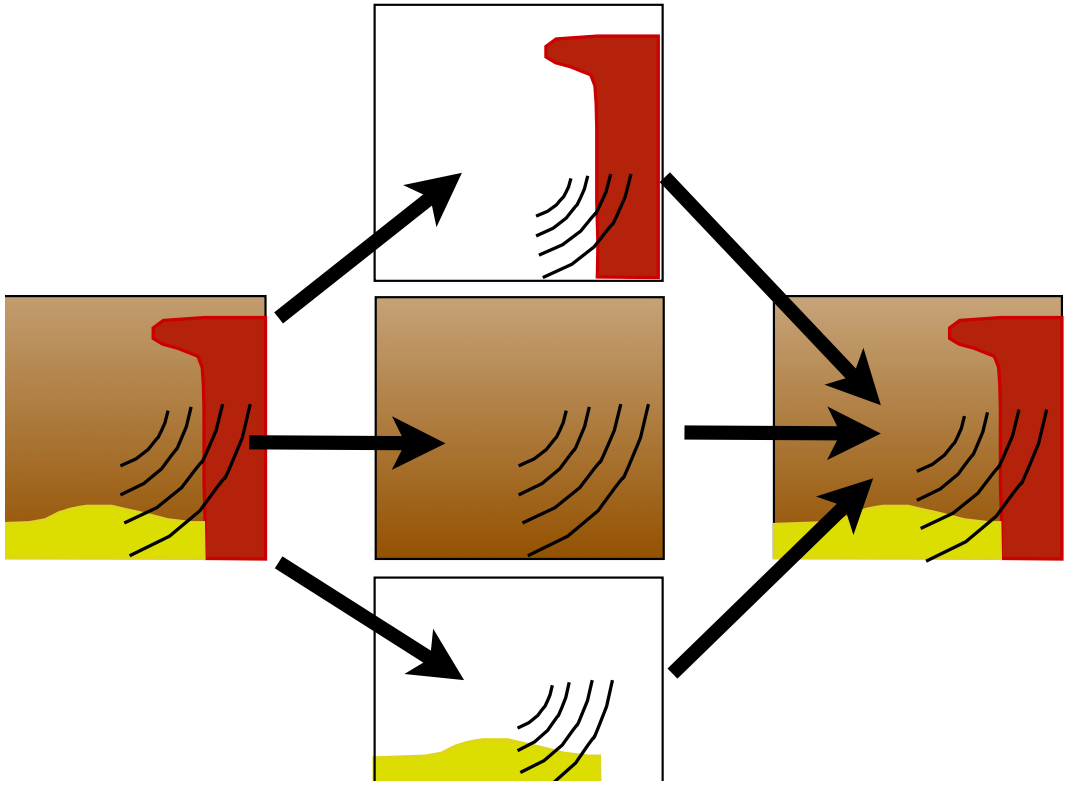

Figure 37: Propagating a wave thru three windowed, irregular regions.

The window breaks up the data into separate streams (e.g. two), each which is processed separately, then recombines

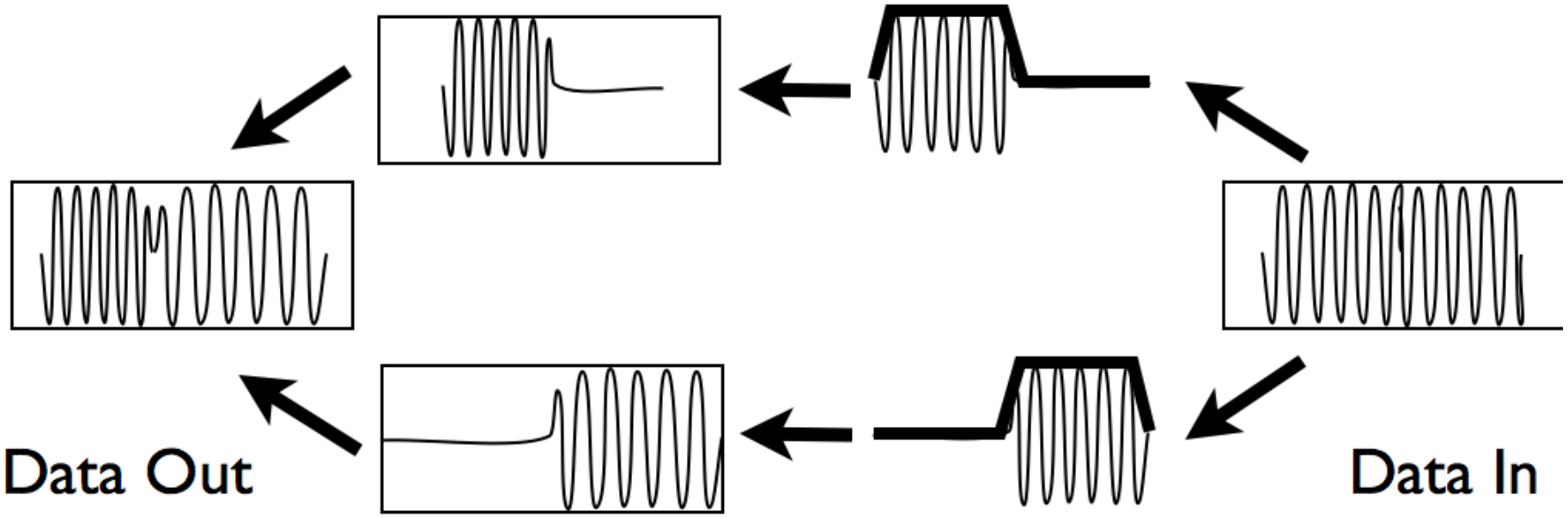

Figure 38: Two windows for data, process, recombine

With many windows, there are many separate streams. Each stream has its own operator, A_k. The dual windows v_k could be different than the w_k.

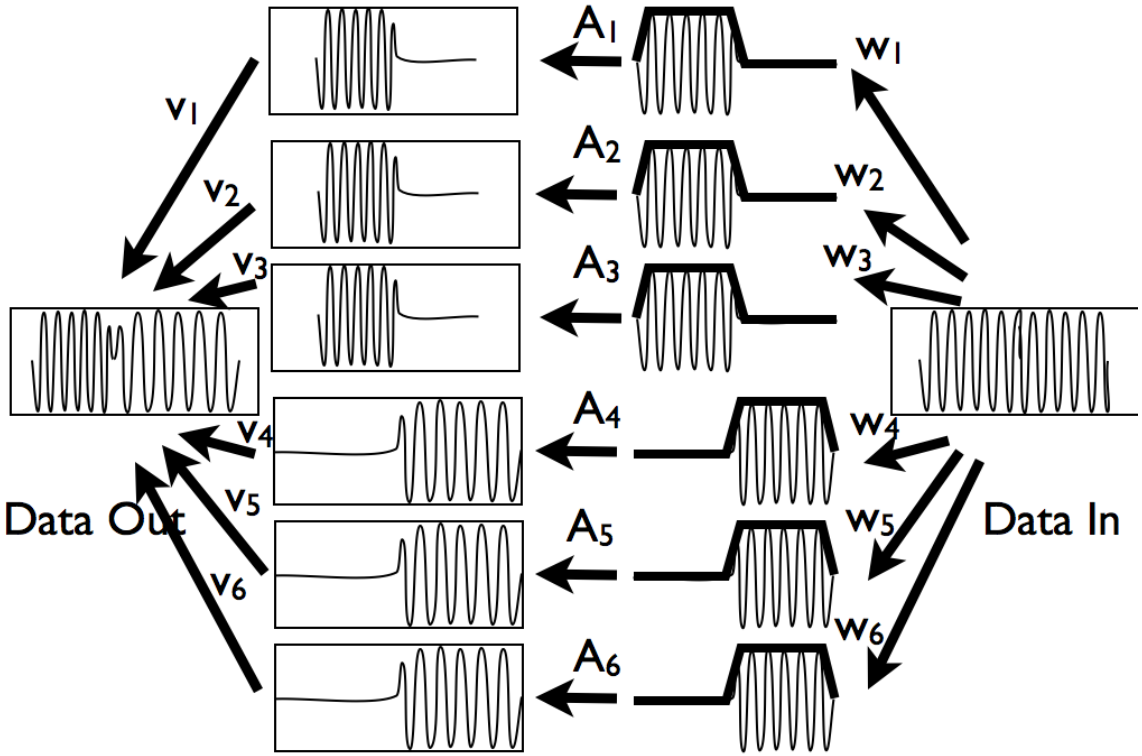

Figure 39: Many windows for data, process, recombine

The data flow is expressed in the form of block matrices acting on signal f,

$$g = \begin{bmatrix} V_1^* & V_2^* & \cdots & V_n^* \end{bmatrix} \begin{bmatrix} A_1 & & & \\ & A_2 & & \\ & & \ddots & \\ & & & A_n \end{bmatrix} \begin{bmatrix} W_1 \\ W_2 \\ \vdots \\ W_n \end{bmatrix} f,$$

where the $W_k = M_{w_k}$ is the windowing operation of multiplication by w_k, V_k for window v_k.

In operator notation, we write

$$g = [V^* A W] f.$$

In summation notation, we write

$$g = \sum_k V_k^* A_k W_k f.$$

This leads to frame theory.

Generalized Frame Theory

Definition 1. *A set of operators* $\{W_1, W_2, \ldots, W_n\}$ *forms a generalized frame if there are constants* $a, b > 0$ *with*

$$a \cdot \mathbb{I} \leq \sum_k W_k^* W_k \leq b \cdot \mathbb{I}.$$

When the W_k operators are multiplication by window functions $w_k(x)$, this definition means

$$a \leq \sum_k |w_k(x)|^2 \leq b, \text{ for all } x.$$

The W_k could give localization in space, in time, or in frequency.

Recall that frame theory works with vectors – in the standard theory, the V_k, W_k are rank on operators. Here we allow larger operators.

Note: the difference between a basis and a frame is redundancy:

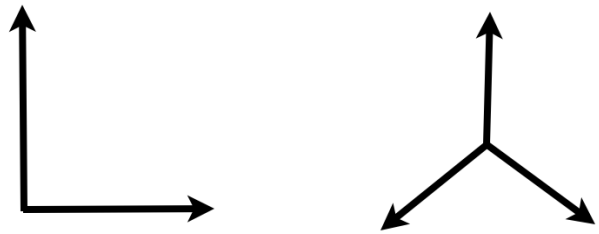

Figure 40: A two-vector basis, and a three-vector frame in $\mathbb{R}^2$.

A frame is a set of vectors that spans a linear space. Typically more vectors than a basis, but with control on the redundancy.

Some typical examples include wavelet, Gabor, curvelet, ridgelet frames.

Frame theory gives algorithms that treat redundancy efficiently.

Standard constructions in Frame theory

Analysis operator $W = [W_1, W_2, \ldots, W_n]^t$

Synthesis operator W^*

Frame operator $S = W^*W$ (positive, invertible)

Normalized frame $\widetilde{W_k} = W_k S^{-1/2}$

Partition of unity (POU) condition

$$\sum_k \widetilde{W_k}^* \widetilde{W_k} = \mathbb{I}$$

Theorem 3. *If the generalized frame $\{W_1, W_2, \ldots, W_n\}$ form a POU, then the operator norms on the windowed operator satisfies*

$$||\sum_k W_k^* A_k W_k|| \leq \max ||A_k||.$$

With window operators $W_1, W_2, \ldots, W_n$ and duals $V_1, V_2, \ldots, V_n$, the partition of unity condition becomes

$$\sum_k \widetilde{V_k}^* \widetilde{W_k} = \mathbb{I}.$$

The corresponding bounds on the norm is not as strong:

Theorem 4. *If the generalized frames $\{W_1, W_2, \ldots, W_n\}, \{V_1, V_2, \ldots, V_n\}$ form a POU, then the operator norms on the windowed operator satisfies*

$$|| \sum_k V_k^* A_k W_k|| \leq \sqrt{n} \max ||A_k||.$$

This is a concern in applications. For instance, one would like to combine localized wave propagators and ensure stability. With a symmetric choice of window, if each A_k a stable propagator, then sum is stable. In many applications, an non-symmetric choice of windows is used. But we could lose stability.

– POU condition on the W_k is important to obtain a functional calculus

– can use pre, post-windows $\{W_1, W_2 \ldots\}$ and $\{V_1, V_2 \ldots\}$ with

$$\sum_k V_k^* W_k = \mathbb{I}.$$

– however, the norm of the combined operator may grow with the number of windows

$$||\sum_k V_k^* A_k W_k|| \approx \sqrt{n} \max ||A_k||$$

which can cause numerical instability.

Example: An unstable wavefield propagator.

By picking windows and shifts just right, one can construct an unstable wave propagator. Here, a stream of five peaks are each windowed, shifted with different local propagators, so the results line up:

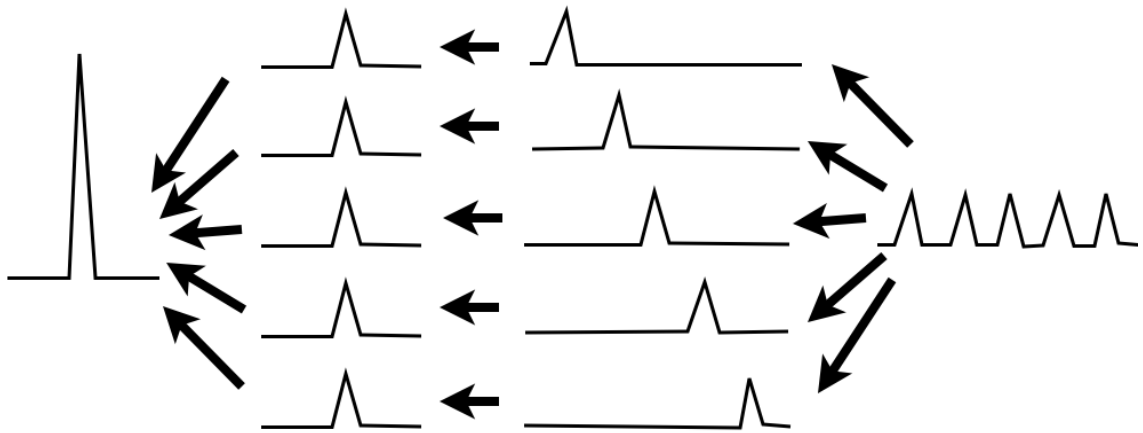

Figure 41: Breaking up a waveform into five, shift just right

Input waveform has energy $\sqrt{1^2 + 1^2 + 1^2 + 1^2 + 1^2} = \sqrt{5}$

Output waveform has energy $\sqrt{5^2} = 5$, increases!

A wavefield propagator

Example: propagate a delta spike through a slow/fast medium, using generalized frames.

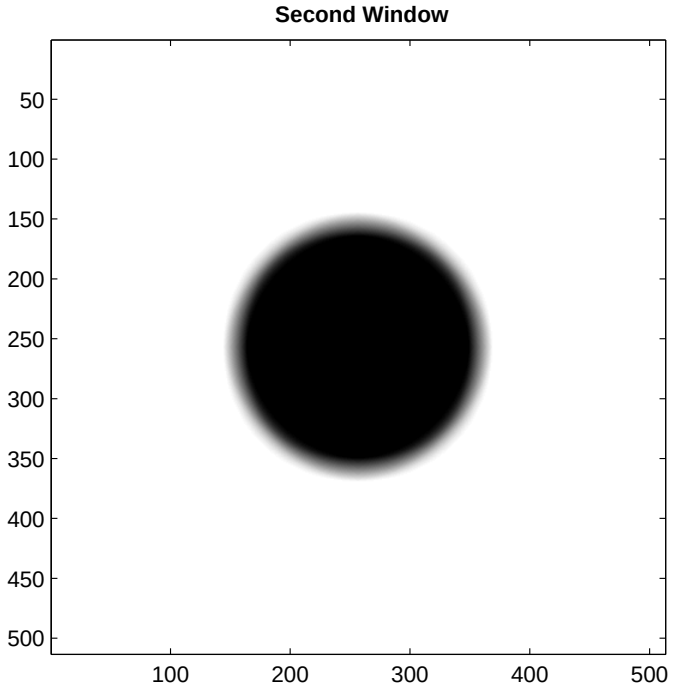

Figure 42: Numerical simulation of seismic propagation.

A breakdown of the numerical simulate: slow (left), fast (middle), total (right).

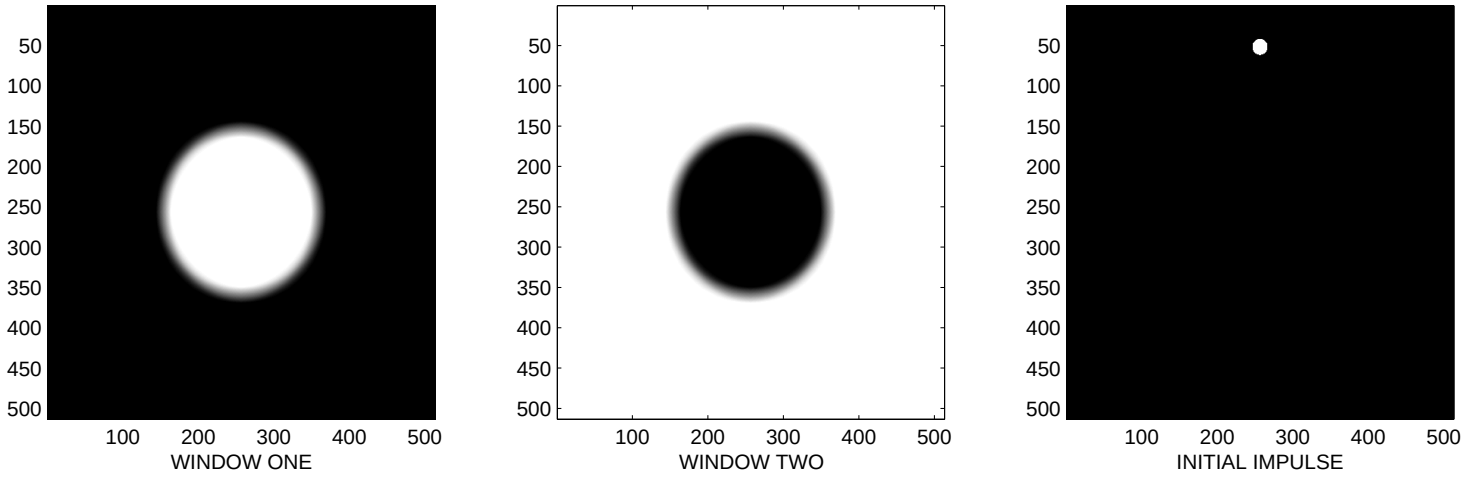

Figure 43: Numerical simulation, two parts summing to the whole.

Goal: try to get as good a result in complex models like Marmousi:

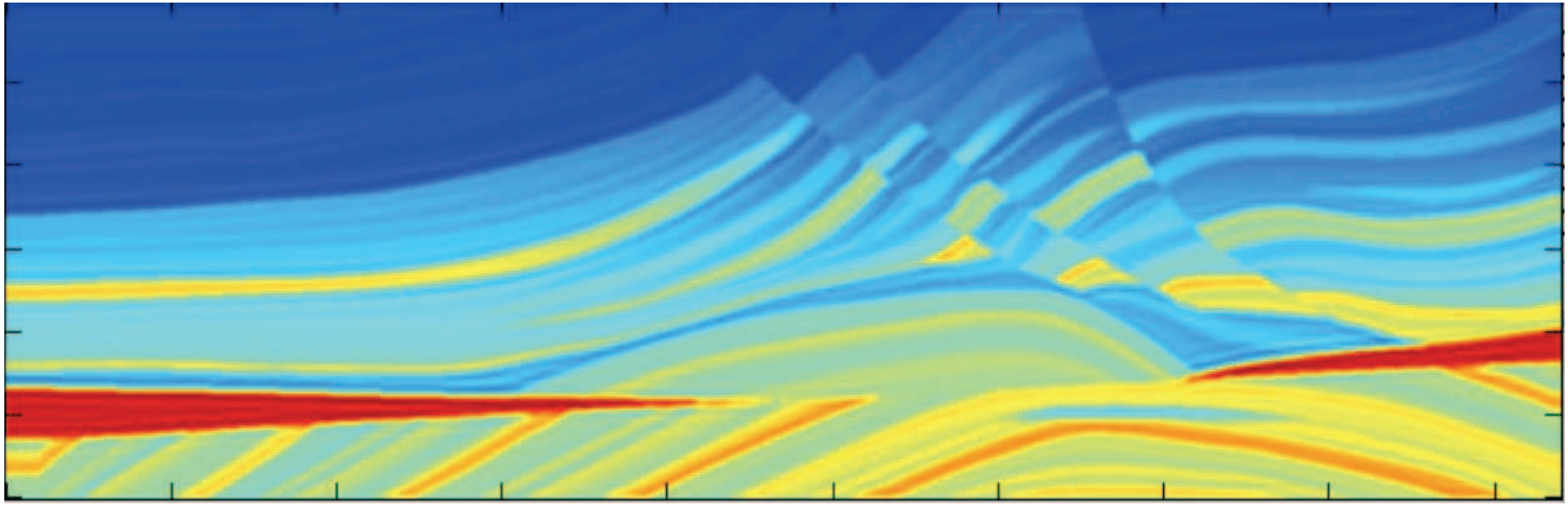

Figure 44: FDTD Simulation of seismic wave propagation through the earth.

Details of the propagation in Marmousi:

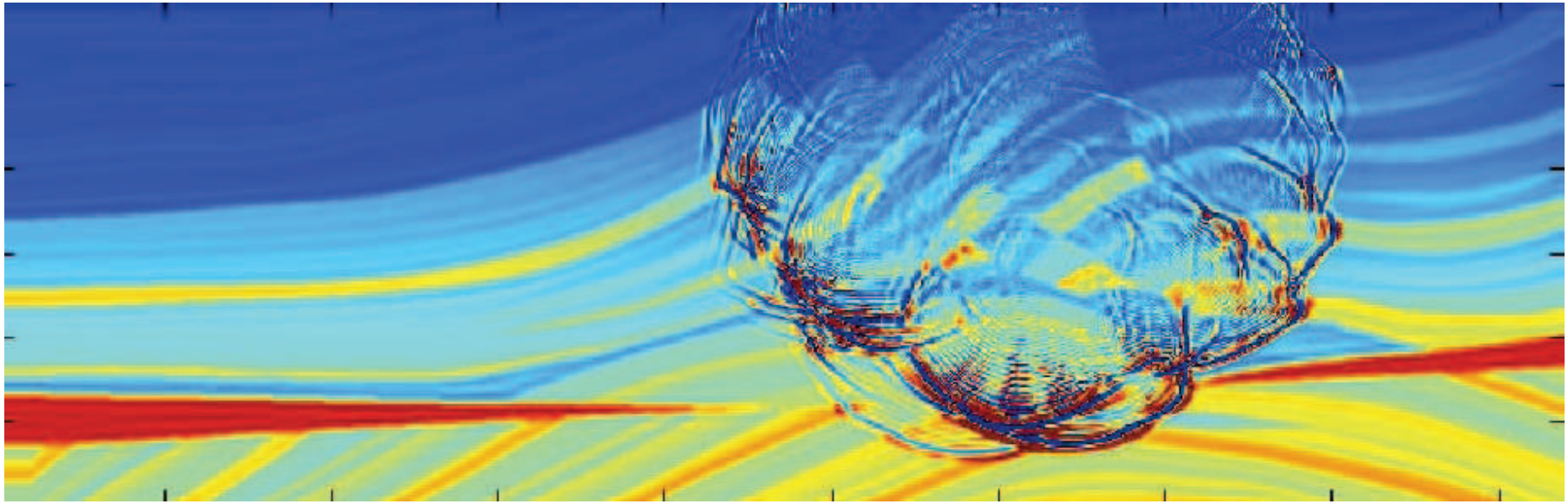

Figure 45: Snapshot: Seismic waves propagating through regions of different velocities.

Discrete Gabor multipliers

Theorem 5. *A discrete Gabor multiplier is a special case of the generalized frame operators.*

Discrete Gabor transform = a discrete time-frequency representation:

$$(\mathcal{G}f)(t_k, \omega) = \int_{\mathbb{R}} f(s) w_k(s-t) e^{-2\pi i s\omega}\, ds.$$

Gabor multiplier = multiplication by function $a = a(t_k, \omega)$ in discrete time-freq domain:

$$f \mapsto \mathcal{G}^* M_a \mathcal{G} f$$

The theorem leads to the expression of this operator as a sum

$$\mathcal{G}^* M_a \mathcal{G} = \sum_k W_k^* C_{a_k} W_k,$$

where the C_{a_k} are convolution operators coming from $a(t_k, \omega)$.

These formulas give simple results for adjoints, and estimates of bounds.

Theorem 6. [Adjoints] *With real symmetric windows ($v_k = w_k$), the adjoint of a discrete Gabor multiplier is obtained by conjugating its symbol:*

$$G_a^* = G_{\overline{a}}.$$

For non-symmetric windows, the analysis and synthesis windows reverse roles in the adjoint of a multiplier:

Theorem 7. [Adjoints] *With non-symmetric windows, $v_k \neq w_k$, the adjoint of a discrete Gabor multiplier is obtained by conjugating its symbol, and reverse order of windows:*

$$G_{a,w,v}^* = G_{\overline{a},\overline{v},\overline{w}}.$$

Theorem 8. [Boundedness] *With symmetric windows, the discrete Gabor multiplier is bounded in norm by its symbol*

$$||G_a|| \leq \sup |a(t_k, \omega)|.$$

For non-symmetric window, the bound can grow:

Theorem 9. [Boundedness] *With non-symmetric windows, v_k, w_k, the discrete Gabor multiplier is bounded by a constant times its symbol*

$$||G_a|| \leq B^{1/2} \sup |a(t_k, \omega)|,$$

where $B = \sup(\sum |v_k|^2) \cdot \sup(\sum |w_k|^2)$.

The Partition of Unity Condition simply states that the square of the windows sum to one.

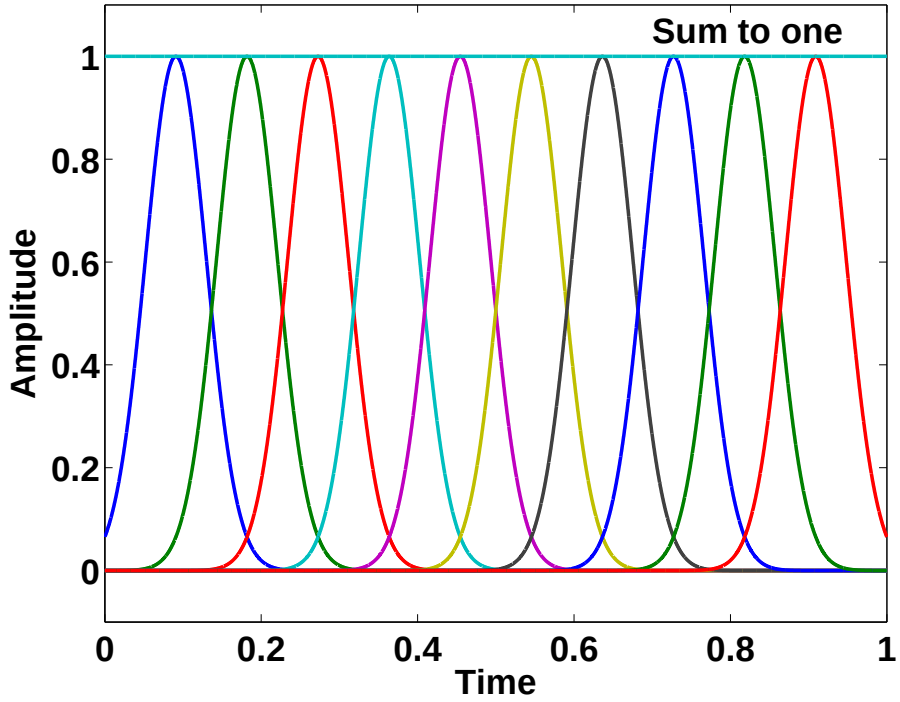

Figure 46: The windows must sum up to one.

One misleading adventure is that Gaussian, when closely spaced, almost sum to one.

Our goal is to formalize a series of approximations, to justify the constructions that appear in Gabor decon and wave field propagators:

$$
\begin{aligned}
\mathcal{G}f &= \text{a discrete time-frequency representation for } f \\
G_1 &= I, \qquad \text{the identity map for a functional calculus} \\
\mathcal{G}(G_a f) &\approx M_a \mathcal{G} f, \qquad \text{action of the multiplier} \\
G_{a+b} &= G_a + G_b \quad \text{sum rule for a functional calculus} \\
G_{a \cdot b} &\approx G_a \cdot G_b \quad \text{product rule} \\
G_{\exp(a)} &\approx \exp(G_a) \quad \text{exponential rule} \\
||G_\alpha||_{op} &\leq ||\alpha||_\infty \quad \text{operator bounds} \\
G_\alpha &\approx K_\alpha, \qquad \text{pseudo-diff approximation}
\end{aligned}
$$

Five of these results are proven; three need work.

Overview of results

Result 1: The convolution theorem

Theorem 10. *The discrete Gabor multiplier G_a is a sum of localized convolutions operators,*

$$G_a = \sum_{k=1}^{M} M_{v_k} C_{a_k} M_{w_k}.$$

The M_{w_k}, M_{v_k} are multiplication by the windows w_k, v_k.

The C_{a_k} is convolution by a_k, where $\mathcal{FT}(a_k)(\omega) = a(x_k, \omega)$.

The windows w_k, v_k come from the forward and inverse transform. Partition of unity condition,

$$\sum_{k=1}^{M} v_k(t) w_k(t) = 1 \qquad \text{for all } t.$$

Result 2. Representing ODEs and PDEs:

For one-sided windows, the Gabor multiplier equals Fourier multiplier, used for constant coefficient differential operators.

For split windows, there is a correction term. Eg: the second order derivative gives

$$\partial_{tt} = G_\alpha + M_d$$

where $d = \sum_k w_k w_k''$ is a correction term.

For an n-th order differential operator, there will be a (n-2)-order differential operator as a correction term.

Result 3. The boundedness theorem

For split windows, positive, matched: $v_m = w_m \geq 0$. Then

Theorem 11. *The norm of the Gabor multiplier G_α satisfies*

$$||G_\alpha|| \leq \max_{x,\xi} |\alpha(x,\xi)|.$$

Eg: a combination of phase shifts will always be energy preserving. The sup norm on the multiplier function α determines a bound on the norm of G_α, as with Fourier multipliers.

Result 4. Combining operators

We have an approximation for the composition of Gabor multipliers

$$G_a G_b \approx G_{a \cdot b}.$$

For boxcar windows, the error term is

$$\Delta = \sum_k M_{w_k} [C_{a_k}, M_{w_k}] C_{b_k} M_{w_k}.$$

A Fourier multiplier composes with a one-way windowed Gabor multiplier,

$$F_a G_b = G_{a \cdot b}$$

and this equality is exact.

Result 5. Approximating PDEs

The Gabor multiplier (with symmetric windows) cannot approximate a 2nd order PDE. However, by adding a correction term of 0-th order, we get an exact representation of a constant coefficient PDE.

For non-constant coefficient, the Gabor representation, with correction term, is approximate to the order of the sup-norm distance between the variable coefficients $a(x), b(x), c(x)$ and their sampled versions $a(x_k), b(x_k), c(x_k)$.

Result 6. Window accuracy

Windowed approximation to the velocity field is accurate to an error no bigger than

$$\frac{v_{max} - v_{min}}{\#\text{ windows}}.$$

Sets the bound on how well the (corrected) Gabor multiplier approximates the PDE.

# of windows sets the speed of computation.

Minimum phase calculations

We've been hiding some details in the Gabor decon, Gabor multiplier results.

Experimentally, one observes that many seismic signals are "minimum phase delay."

Roughy speaking, this means energy is concentrated near the start of the signals.

Examples: A dynamite blast. A weight drop. A Vibroseis sweep, after attenuation.

Observation: As a signal travels through the earth, minimum phase in yields minimum phase out.

Consequence: Any reasonable numerical model must have the property of preserving minimum phase. This includes our Gabor multipliers.

It helps to start with a precise definition of minimum phase:

Theorem 12. [Complex analysis] *A sampled signal* $f = (f_0, f_1, f_2, \ldots)$ *in* l^2 *is minimum phase if and only if its z-transform*

$$F(z) = \sum_k f_k z^k$$

is an outer function in the Hilbert-Hardy space $H^2(\mathbb{D})$*.*

That is, the analytic function $F(z)$ is determined by its absolute value on the boundary of the disk,

$$F(z) = \lambda \cdot \exp\left(\frac{1}{2\pi}\int_{-\pi}^{\pi} \frac{e^{i\theta}+z}{e^{i\theta}-z} \log|F(e^{i\theta})|\, d\theta\right),$$

up to a constant λ of modulus one.

Equivalently, the sample signal $f = (f_0, f_1, f_2, \ldots)$ is determined by the amplitude of its Fourier transform (up to a constant).

Our ears can hear the difference: these three signals have the same amplitude spectrum.

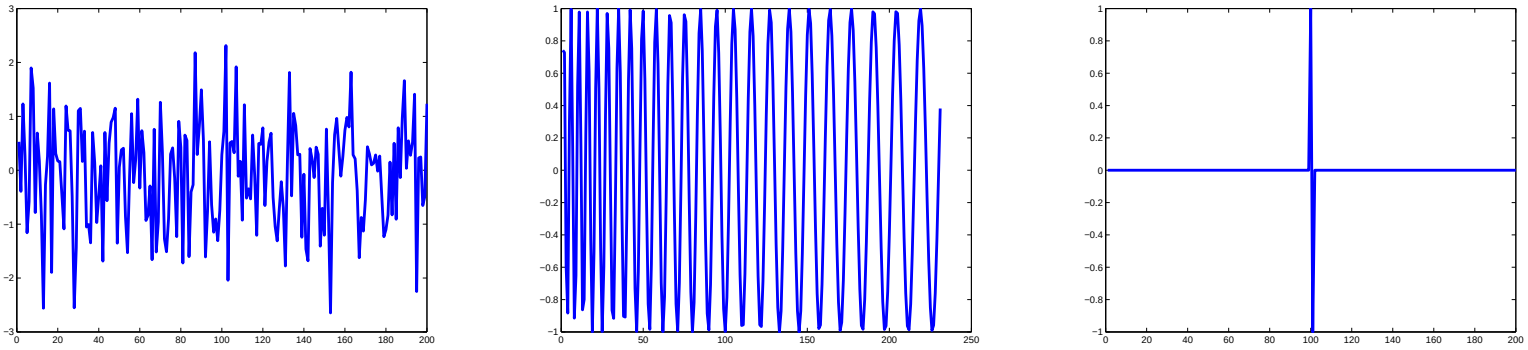

Figure 47: **Some noise**, **a singular sweep**, **a Dirac delta pulse**.

Theorem 13. [Gibson-L-Margrave, 2011] *Let* $A : H^2(\mathbb{D}) \longrightarrow H^2(\mathbb{D})$ *be a bounded linear operator, preserving the set of outer functions. Then there exists some outer function* ψ*, and analytic function* $\phi : \mathbb{D} \longrightarrow \mathbb{D}$ *such that*

$$(AF)(z) = \psi(z)F(\phi(z)), z \in \mathbb{D}$$

for all functions F in $H^2(\mathbb{D})$.

That is, the only outer preserving operators have a very simple form – multiplication by outer function ψ, and composition with analytic function ϕ.

The functions ψ, ϕ have a physical meaning. ψ represents a stationary filter (e.g. coupling between dynamite and earth). ϕ represents a frequency dependent decay, which is exponential in both time and frequency parameter.

$$\exp(-t\omega/Q(\omega)).$$

We get Q-attenutation for free!

This is connected to a deep result on linear maps of polynomials preserving certain zero sets. Let given a set Ω in the complex plane, let $\mathcal{P}(\Omega)$ denote the set of polynomials which are non-zero on Ω. We have the following:

Theorem 14. [Gibson-L-Margrave, 2011] *Suppose Ω_1 is bounded, Ω_2 has non-empty interior. A linear map A on polynomials has property $A(\mathcal{P}(\Omega_1)) \subset \mathcal{P}(\Omega_2)) \cup \{0\}$ if and only if either:*

- *there is a linear functional ν and polynomial $\psi \in \mathcal{P}(\Omega_2)$ with $A(p) = \nu(p)\psi$, or*
- *there are polynomials ψ, ϕ such that $\psi \in \mathcal{P}(\Omega_2), \phi(\Omega_2) \subset \Omega_1$, with $A(p) = \psi \cdot (p \circ \phi)$.*

This is a constructive solution to the Pólya-Schur problem on polynomials, extending some recent results by Borcea and Brädén. The proof depends on properties of a constructed entire function generated by the operator A.

In sampled signal space, the minimum phase preserve operators are described precisely as lower triangular matrices of a special form. Each column corresponds to the coefficients in the Taylor series expansion of the function $\psi(z)\phi^n(z)$.

In particular, the first two columns are enough to determine the whole matrix for the operator. Consequently, two measurements of delta impulses is enough to determine the operator.

Problem: this is a very restrictive class of operators. It suggests the minimum phase assumption is too strong – it may be appropriate to use a more local version of minimum phase preservation. Or perhaps the identification with time-to-space is inappropriate.

Summary

Time-frequency representations lead naturally to multipliers.

We focus on the Gabor multipliers, for reasons of speed, and useful experience. Other time-frequency representations could lead to useful multipliers.

Gabor multipliers approximate pseudo differential operators. Numerically, we get useful operators to model wave propagation.

Generalized frame theory is useful to analyze the discrete Gabor multipliers.

We can model physically important phenomenal including non stationary convolution, deconvolution, wave propagation, and minimum phase preserving linear operators.

Acknowledgements

Special thanks to:

- collaborators Elise Fear, Peter Gibson, Gary Margrave, and our students
- the industry sponsors of CREWES and POTSI
- the research agencies MITACS, MPrime, NSERC, PIMS

References

Gibson, Lamoureux, 2012. *Identification of minimum-phase-preserving linear operators on the half-line*, Inverse Problems.

Gibson, Lamoureux, Margrave, 2012. *Representation of Linear Operators by Gabor Multipliers*, in "Excursions in Harmonic Analysis: The February Fourier Talks at the Norbert Wiener Center," Applied and Numerical Harmonic Analysis (Birkhauser).

Gibson, Lamoureux, Margrave, 2011. *Outer preserving linear operators*, Journal of Functional Analysis.

Margrave, Lamoureux, Henley, 2011. *Gabor deconvolution: Estimating reflectivity by nonstationary deconvolution of seismic data*, Geophyiscs.

Feichtinger, Helffer, Lamoureux, Lerner, Toft, 2008, *Pseudo-Differential Operators, Quantization and Signals*, Springer Lecture Notes in Mathematics, Vol. 1949.

Margrave, Lamoureux, 2006. *Gabor Deconvolution*, The Recorder, special edition, Can. Soc. of Expl. Geophys.

Lamoureux, Margrave, 2006. *An Introduction to Numerical Methods of Pseudodifferential Operators*, Proceedings of the CIME Workshop on Pseudodifferential Operators, Quantization and Signals.

Margrave, Geiger, Al-Saleh, Lamoureux, 2006. *Improving explicit seismic depth migration with a stabilizing Wiener filter and spatial resampling*, Geophysics.

Lamoureux, 2005. *Seismic image analysis using local spectra*, Canadian Applied Mathematics Quarterly.

Margrave, Gibson, Grossman, Henley, Iliescu, Lamoureux, 2004. *The Gabor transforms, pseudodifferential operators, and seismic deconvolution*, Integrated Computer-Aided Engineering.

Margrave, Dong, Gibson, Grossman, Henley, Lamoureux, 2003. *Gabor deconvolution: extending Wiener's method to nonstationarity*, The CSEG Recorder.